

Mono- and Dinuclear α -Diimine Nickel(II) and Palladium(II) Complexes in C–S Cross-Coupling

Md Muktadir Talukder, Justin T. Miller, John Michael O. Cue, Chinthaka M. Udamulle, Abhi Bhadrar, Michael C. Biewer, and Mihaela C. Stefan*



Cite This: <https://dx.doi.org/10.1021/acs.organomet.0c00732>



Read Online

ACCESS |



Metrics & More

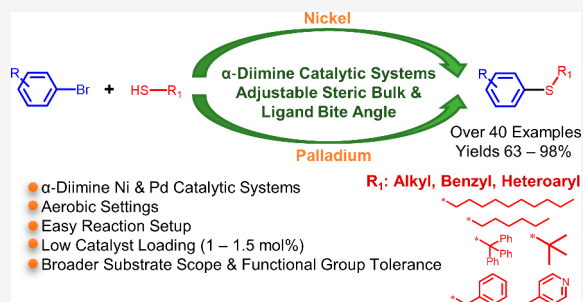


Article Recommendations



Supporting Information

ABSTRACT: The usefulness of transition metal catalytic systems in C–S cross-coupling reactions is significantly reduced by air and moisture sensitivity, as well as harsh reaction conditions. Herein, we report four highly air- and moisture-stable well-defined mononuclear and bridged dinuclear α -diimine Ni(II) and Pd(II) complexes for C–S cross-coupling. Various ligand frameworks, including acenaphthene- and iminopyridine-based ligands, were employed, and the resulting steric properties of the catalysts were evaluated and correlated with reaction outcomes. Under aerobic conditions and low temperatures, both Ni and Pd systems exhibited broader substrate scope and functional group tolerance than previously reported catalysts. Over 40 compounds were synthesized from thiols containing alkyl, benzyl, and heteroaryl groups. Also, pharmaceutically active heteroaryl moieties are incorporated from thiol and halide sources. Notably, the bridged dinuclear five-coordinate Ni complex has outperformed the remaining three mono four- or six-coordinate complexes by giving almost quantitative yields across a broad substrate scope.



INTRODUCTION

Numerous innovative synthetic methods have arisen from the desire to form carbon–heteroatom bonds through transition metal catalysts.^{1,2} C–S bond formation remains one of the most valuable chemical transformations for pharmaceutical applications.^{3,4} The first transition-metal-catalyzed C–S cross-coupling reaction between thiols and aryl halides was reported by Migita et al. using Pd(PPh₃)₄.^{5,6} Subsequently, extensive studies have been performed using Pd^{7–16} and other transition metals, including Co,¹⁷ Ni,^{18–25} Cu,^{26–28} Rh,²⁹ and In.³⁰

Pd-catalyzed systems have been extensively studied but suffer from several issues. Deactivation of Pd catalysts through off-cycle thiolate complexes significantly reduces their efficacy.^{8,13} Additionally, systems for *in situ* catalyst generation suffer from expensive precursors.⁸ Recently, Ni-based systems have gained popularity for their environmental friendliness, cost-effectiveness, and decreased tendency to deposit metallic nanoparticles.³¹ However, both Pd- and Ni-catalytic systems continue to demand high catalyst loading (5–50 mol %),^{8,18,22–25,31} high temperature (100–150 °C),^{7,9,11,12,15,16,23,31} expensively designed ligands,^{3,17} additives,^{20,23,24} and longer reaction times (12–72 h).^{7–9,11–13,15,18,23,25,29,31} Previously reported systems that do well concerning these issues, such as Venkanna et al.'s Ni-pyrrole system or Buchwald et al.'s Pd-monophosphine system, still suffer from the requirement of using glovebox conditions.^{14,19} Consequently, harsh reaction conditions significantly hinder the C–S coupling of alkyl-substituted thiols^{20,32}

and pharmaceutically important heterocycles.^{14,33} Photoredox catalysis has attracted attention as a possible solution, but widely used iridium- and ruthenium-based photosensitizers are expensive and have inadequate substrate scope.²²

To overcome the existing challenges in transition-metal-catalyzed C–S coupling, the influence of steric topography around the metal center and the ligand bite angle has been studied. For instance, promoting oxidative addition and reductive elimination through higher steric bulk and ligand bite angle significantly reduces the off-cycle thiolate complexes.^{9–13} Moreover, Scattolin et al. have reported a bridged dinuclear Pd catalyst in C–S cross-coupling that displayed promising performance by preventing off-cycle thiolate complexes.⁸ In light of these factors, α -diimine-based transition metal catalysts represent an excellent candidate for C–S cross-coupling due to tunable sterics and bite angles. Olefin polymerization was revolutionized through the introduction of Brookhart-type α -diimine transition metal catalysts, bringing facile synthesis, structural versatility, high thermal stability as well as air and moisture stabilities.^{34–36} In addition, electronic and steric features, including the ligand bite angle, are

Received: November 17, 2020

adjustable by incorporating various functional moieties in the ligand structure.^{34,37,38}

In a recent publication, we have demonstrated a series of α -diimine Ni(II) and Pd(II) complexes for C–C bond formation through the Suzuki–Miyaura cross-coupling reaction.³⁴ Both iminopyridine- and acenaphthene-based ligand frameworks were implemented to synthesize mono- and dinuclear Ni(II) and Pd(II) complexes for investigating the steric features in the catalytic performance. Also, sterically challenging boronic acids were incorporated with a wide variety of aryl halides containing reactive functionalities. However, the highest steric bulk associated with the five-coordinate bridged-dinuclear Ni(II) exceeded the remaining four- or six-coordinate mononuclear complexes regarding the catalytic performance. Here, we have investigated the promising features of α -diimine transition metal complexes in C–S cross-coupling (Figure 1). We report

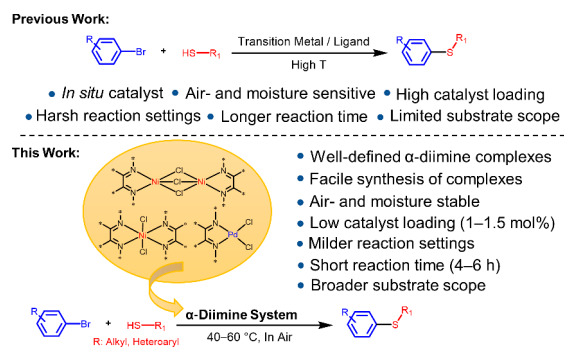


Figure 1. Overview of transition-metal-catalyzed C–S cross-coupling.

the first application of mono- and dinuclear Ni(II) and Pd(II) complexes in C–S cross-coupling. Acenaphthene- and iminopyridine-based ligands were applied to synthesize the Ni(II) and Pd(II) complexes. Variation in the steric features was analyzed and correlated to the reaction outcomes. Notably, significant consideration was given to examine the substrate scope through the coupling of thiols containing heteroaryl or alkyl moieties with various aryl halides.

RESULTS AND DISCUSSION

Synthesis and Characterization of α -Diimine Nickel(II) and Palladium(II) Complexes. Synthesis and structural characterization of the complexes are displayed in Scheme 1. The ligands and complexes were synthesized by adopting a reported procedure.³⁴ Iminopyridine- (1a, 1b, and 1d) and acenaphthene-based (1c) ligands were prepared through condensation reactions of primary arylamines, 2-pyridine carboxaldehyde, and acenaphthoquinone, respectively. Two equivalents of the ligand 1a with NiCl₂(DME) afforded the mononuclear bis-ligated complex, Ni A-1, whereas 1 equiv of ligand 1d generated the dinuclear monoligated complex, Ni B-1. The remaining two mononuclear Pd(II) complexes, Pd A-1 and Pd B-1, were synthesized by reacting the ligands 1b and 1c with 1 equiv of PdCl₂(COD), respectively. Scheme 1 shows the ORTEP diagrams of the synthesized complexes. Distorted octahedral geometry was observed for both Ni A-1 and Ni B-1. For Ni A-1, the nickel atom is coordinated by two free chlorine atoms and four nitrogen atoms of the iminopyridine ligands. It has some positional disorder resulting from the phenyl ring bearing the butyl substituent; however, this does not significantly alter the packing of the complex in the solid

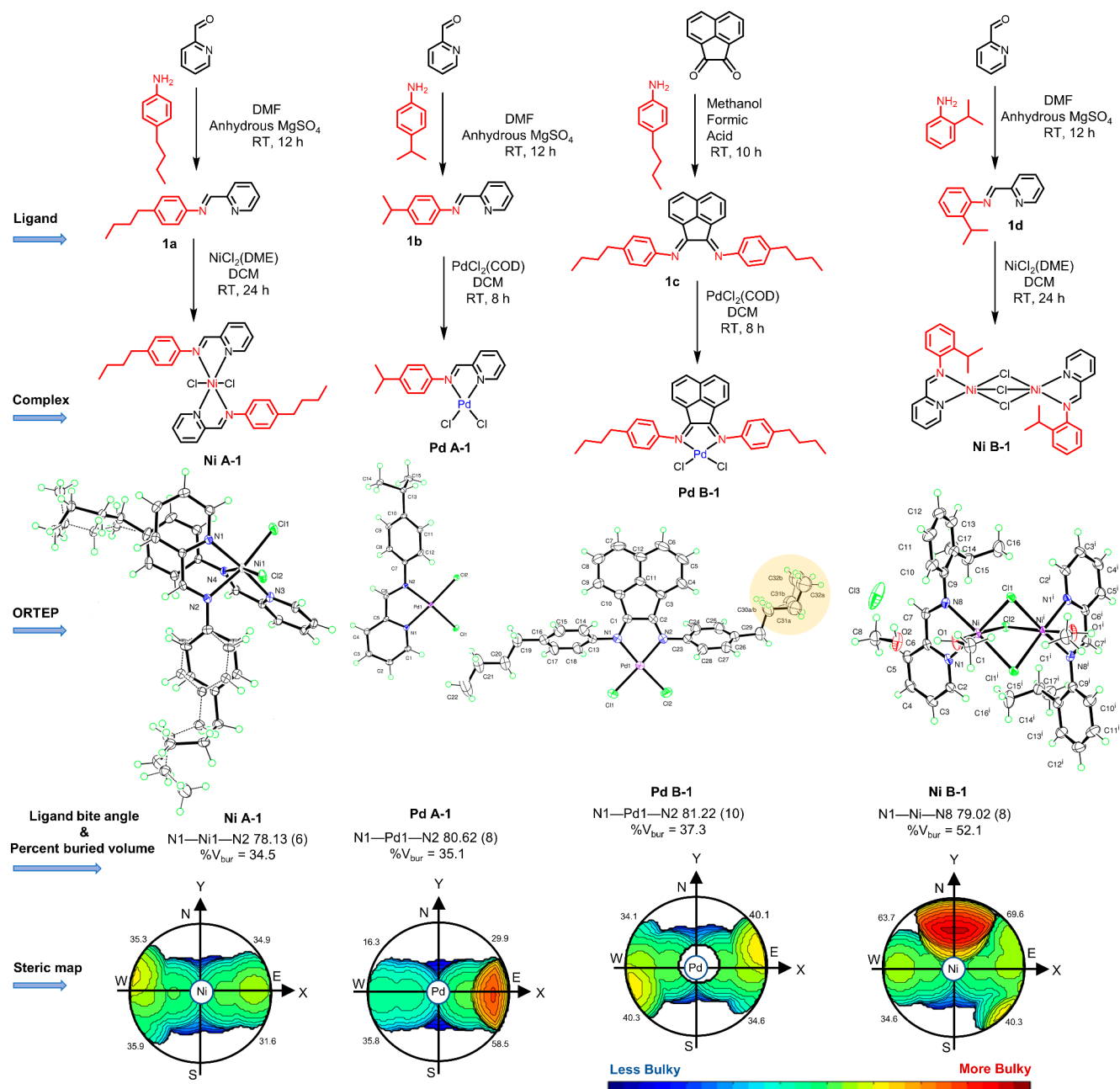
state. Ni B-1 is a centrosymmetric dimer with an octahedral geometry about each of the two nickel centers. Two nitrogen atoms arising from the ligand are directly coordinated with each of the nickel centers and three bridging chlorine atoms. A methanol molecule from the solvent used in crystal growth is coordinated to each Ni center. In addition, one free methanol and a chloride anion are present in the structural packing of Ni B-1. Meanwhile, Pd A-1 and Pd B-1 exhibit a distorted square planar geometry with two nitrogen atoms from the ligand that are directly coordinated with the Pd center along with two free chlorine atoms. Pd B-1 has some positional disorder from one of the butyl chains. Unit cell representations, crystal data collection, selected bond angles, and distances are provided in the Supporting Information.

Reaction Conditions Optimization in C–S Cross-Coupling. Both Ni- and Pd-based catalytic systems are established through Ni A-1 and Pd A-1, respectively. For this purpose, 0.5 mol % of these complexes was employed with 2-bromonaphthalene (2a) and 1-hexanethiol (2b). The base, solvent, and temperature were screened by running the reaction with a molar ratio of 2a and 2b as 1:1.5 (Table 1). At 40 °C, nine experiments (Table 1, entries 1–9) were executed to find the best solvent and base combination for both Ni A-1 and Pd A-1 catalytic systems. Water and NaOH provided the best yield for Pd A-1, whereas 1,4-dioxane and KOH for Ni A-1 (Table 1, entries 5 and 7). Another five experiments were performed from 30 to 80 °C for finding the optimum temperature (Table 1, entries 10–14). Comparing to the previously obtained highest yield for Ni A-1 (Table 1, entry 7), altering the temperature did not improve the performance (Table 1, entries 10–14). On the other hand, Pd A-1 generated the best yield by increasing the temperature to 60 °C (Table 1, entry 10).

Another set of experiments was performed to identify the optimum concentration of complexes. In addition, the ratio of 2a and the base at different times was analyzed for finding the optimum conditions (Table 2). At 0.5 mol % of complexes, both Ni A-1 and Pd A-1 gave an increase in yields by changing the ratio of 2a and the base from 1:1.2 to 1:1.5; however, a decrease was observed when using a 1:1.8 ratio (Table 2, entries 1 and 2). With the optimized conditions, Pd A-1 provided the highest yield (94%) from using 1.5 mol % of the complex for 4 h, whereas 1 mol % of the complex for 6 h afforded the best yield (89%) for Ni A-1 (Table 2, entries 4 and 6). There was no background reactivity observed without the employment of synthesized Ni A-1 and Pd A-1 catalysts under the employed conditions (Table 2, entries 10 and 11).

Evaluation of the Complexes in C–S Cross-Coupling. Percent buried volume (%V_{bur}) is used as a molecular descriptor for estimating the catalytic performance of the complex in C–S cross-coupling. %V_{bur} has been used for quantifying the steric attributes of various catalysts.^{34,39,40} Here, we have used SambVca 2.1, a free web application designed by Falivene et al., to produce the topographic steric maps and calculate the %V_{bur} of the complexes (Scheme 1).⁴⁰ Ni A-1 exhibits the lowest buried volume (%V_{bur} = 34.5) and ligand bite angle (N1–Ni1–N2 = 78.13(6)°). Pd A-1 has a higher buried volume (%V_{bur} = 35.1) and ligand bite angle (N1–Pd1–N2 = 80.62(8)°) than Ni A-1. Pd B-1, having an acenaphthene-based symmetrical ligand structure, shows a notable increase in the buried volume (%V_{bur} = 37.3) and ligand bite angle (N1–Pd1–N2 = 81.22(10)°). The bridged dinuclear Ni B-1 complex has a lower bite angle (N1–Ni–N8

Scheme 1. Synthesis, ORTEP Diagrams, Ligand Bite Angle, Percent Buried Volume, and Steric Maps of the α -Diimine Ni(II) and Pd(II) Complexes

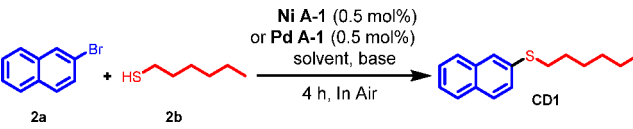


= 79.02(8)°; however, it has the highest buried volume ($\%V_{\text{bur}} = 52.1$) of the synthesized complexes.

$\%V_{\text{bur}}$ and ligand bite angles of the complexes are examined for correlation with the reaction outcomes (Scheme 1). For this purpose, nine compounds were synthesized by applying each of the four complexes (Scheme 2). Thiols containing alkyl, benzyl, and heteroaryl moieties were reacted with aryl or heteroaryl bromides. Generally, the bridged dinuclear Ni B-1 complex provided the highest yields. Pd B-1 was superior to the Pd A-1 and Ni A-1, whereas Ni A-1 exhibited the lowest yields. The difference in the catalytic performance is more significant in the compounds containing heteroaryl moieties (Scheme 2, CD6–CD9). Greater steric bulk and ligand bite angle facilitates the reductive elimination and oxidative addition.^{9–13} Moreover, reductive elimination is promoted by

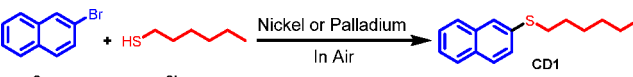
greater orbital overlap due to a wider bite angle.^{34,41} Accordingly, Pd A-1, possessing a higher $\%V_{\text{bur}}$ and ligand bite angle, affords better yields than Ni A-1. For understanding the improved performance of Pd B-1, similar observations are relevant. Noticeably, the bridged dinuclear Ni B-1, with an overwhelming amount of steric bulk, has outperformed the remaining three mononuclear complexes.

Off-cycle thiolate complexes are responsible for diminishing the catalytic performance of transition metal complexes in C–S cross-coupling.^{8,13} A dinuclear Pd complex overcomes this shortcoming by preventing the formation of off-cycle complexes.⁸ Higher nucleophilicity emerging from the smaller size of Ni(0) compared to Pd(0) promotes oxidative addition.³⁴ Moreover, in reductive elimination, the six-coordinate complex generates a five-coordinate intermediate

Table 1. Optimization of the Base, Solvent, and Temperature^a


entry	temp (°C)	solvent	base	yield (%) ^b (Ni A-1/Pd A-1)
1	40	DMF	KOH	22/33
2	40	DMF	NaOH	22/65
3	40	DMF	K ₂ CO ₃	43/57
4	40	H ₂ O	KOH	34/49
5	40	H ₂ O	NaOH	40/66
6	40	H ₂ O	K ₂ CO ₃	47/51
7	40	1,4-dioxane	KOH	58/51
8	40	1,4-dioxane	NaOH	42/58
9	40	1,4-dioxane	K ₂ CO ₃	19/50
10	30	H ₂ O	NaOH	36/61
11	60	H ₂ O	NaOH	33/71
12	80	H ₂ O	NaOH	27/63
13	30	1,4-dioxane	KOH	41/47
14	60	1,4-dioxane	KOH	36/49

^aReaction conditions: 2-bromonaphthalene (2a) (1 mmol), 1-hexanethiol (2b) (1.5 mmol), base (1.2 mmol), 0.5 mol % of Ni A-1 or Pd A-1, and solvent (5 mL). ^bIsolated yields after silica gel column chromatography.

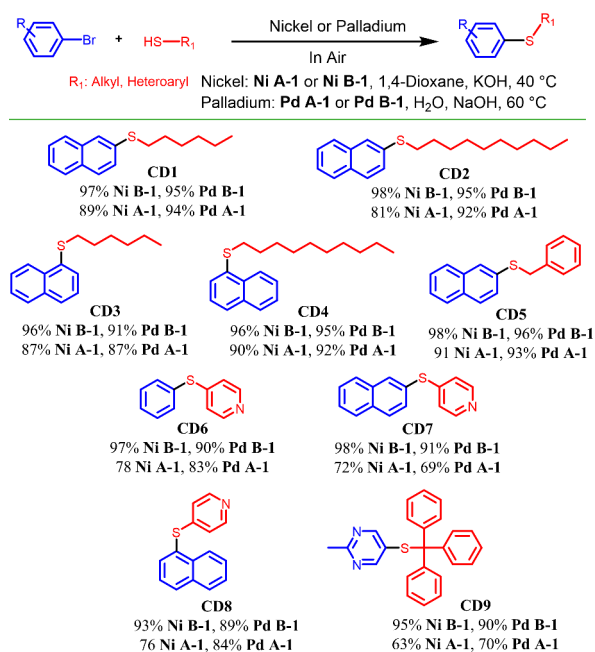
Table 2. Optimization of Time, Concentration of Complex, and Halide/Base Ratios^a


entry	time (h)	conc. (mol %)	halide/base	yield (%) ^b (Ni A-1/Pd A-1)
1	4	0.5	1/1.5	65/83
2	4	0.5	1/1.8	56/77
3	4	1	1/1.5	81/89
4	4	1.5	1/1.5	73/94
5	4	2	1/1.5	-/91
6	6	1	1/1.5	89/87
7	8	1	1/1.5	78/-
8	6	1.5	1/1.5	69/88
9	3	1.5	1/1.5	65/79
10	6		1/1.5	0/-
11	4		1/1.5	-/0

^aReaction conditions: 2-bromonaphthalene (2a) (1 mmol), 1-hexanethiol (2b) (1.5 mmol), base, Ni A1 or Pd A1, and solvent (5 mL). ^bIsolated yields with silica gel column chromatography. Entry 5 for only Pd A-1; entry 7 for Ni A-1 only. Entries 10 and 11 without Ni A-1 and Pd A-1, respectively, through GC–MS.

through ligand loss rather than the direct coupling compared to a five-coordinate complex.⁴² Accordingly, without the coordinated solvent methanol, the bridged dinuclear five-coordinate Ni B-1 complex has outperformed the remaining three mononuclear four- or six-coordinate complexes in the reaction performance.

Expansion of Substrate Scope: Aromatics. Two promising complexes, Ni B-1 and Pd B-1, were selected for expansion of substrate scope in C–S cross-coupling (Scheme 3). Various primary and tertiary alkyl thiols and benzyl thiols

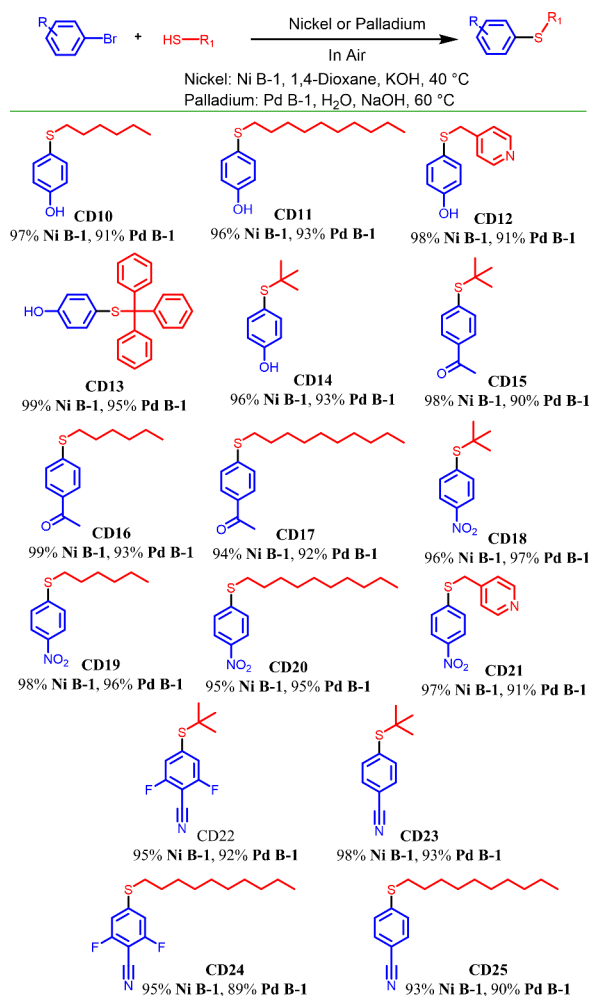
Scheme 2. Evaluation of the Complexes in C–S Cross-Coupling^a

^aNickel: Aryl halide (1 mmol), thiol (1.5 mmol), KOH (1.5 mmol), 1,4-dioxane (5 mL), 1 mol % of complex Ni A-1 or Ni B-1 for 6 h at 40 °C. Palladium: Aryl halide (1 mmol), thiol (1.5 mmol), NaOH (1.5 mmol), H₂O (5 mL), 1.5 mL of complex Pd A-1, or Pd B-1 for 4 h at 60 °C. Isolated yields from column chromatography.

were reacted with aryl bromides for synthesizing 16 compounds carrying a hydroxyl, acetyl, nitro, and nitrile functionality. Ni B-1 outperformed Pd B-1 with nearly quantitative yields, whereas Pd B-1 afforded lesser, but still excellent, yields.

Aryl halides containing hydroxyl groups are challenging to couple with thiols because they often need to be protected with a silyl group.¹⁶ However, in our attempts, without protecting the hydroxyl group, high yields were recorded from 4-bromophenol and different alkyl thiols. For instance, thiols containing *tert*-butyl or bulkier triphenylmethyl moieties gave comparable yields. Aryl halides having a reactive acetyl functionality are another class of compounds that often result in low C–S cross-coupling yields with alkyl thiols.³² Nonetheless, introducing an acetyl functionality through 4-bromoacetophenone and alkyl thiols did not significantly adversely impact Ni B-1 and Pd B-1 catalytic systems, which continued to deliver excellent to quantitative yields.

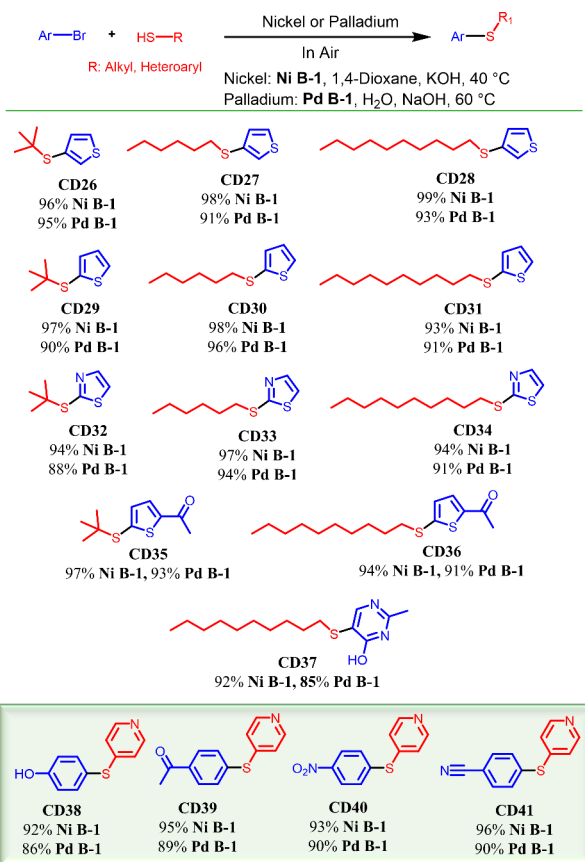
Nitroaromatic compounds are useful building blocks for nucleophilic aromatic substitution. Alkylation of nitroaromatic compounds through C–C cross-coupling is achieved by utilizing pyrophoric organometallic reagents such as butyllithium.⁴³ C–S cross-coupling allows a more desirable way to produce the alkyl thiolated nitroaromatic compounds. We have employed alkyl and benzyl thiols for alkyl thiolation of 1-bromo-4-nitrobenzene, obtaining yields of 91–98%. Aryl nitriles are biologically active organic compounds found in pharmaceuticals and natural products. A nitrile functionality can install other useful functionalities, including amines, aldehydes, and acid derivatives.⁴⁴ Here, we have synthesized four alkyl thiolated benzonitriles through Ni B-1 and Pd B-1 systems with excellent yields. Both 4-bromobenzonitrile and 4-

Scheme 3. Expansion of Substrate Scope: Aromatics^a

^a**Nickel:** Aryl halide (1 mmol), thiol (1.5 mmol), KOH (1.5 mmol), 1,4-dioxane (5 mL), 1 mol % of complex Ni B-1 for 6 h at 40 °C. **Palladium:** Aryl halide (1 mmol), thiol (1.5 mmol), NaOH (1.5 mmol), H₂O (5 mL), 1.5 mL of complex Pd B-1 for 4 h at 60 °C. Isolated yields from column chromatography.

bromo-2,6-difluorobenzonitrile are coupled with *tert*-butylthiol with similar yields.

Expansion of Substrate Scope: Heteroaromatics. The field of organic electronics heavily depends on the five-membered heteroaryl compounds. Alkylated thiophene and thiazole moieties are essential building blocks for designing photovoltaic materials.^{45,46} Alkylthiol side chains have been shown to improve the optoelectronic properties of conjugated polymers.⁴⁷ We have synthesized 11 compounds containing different alkyl thiol side chains on the thiophene and thiazole units (Scheme 4, CD26–CD36). These useful compounds have the potential to be utilized as building blocks for organic semiconducting materials. Through Ni B-1 and Pd B-1, we have obtained good to quantitative yields (88–99%) for alkylthiolation of 2-bromothiophene, 3-bromothiophene, and 2-bromothiazole with various alkyl thiols. Nitrogen as an additional heteroatom in the thiazole unit did not significantly decrease the yields compared to the one heteroatom in thiophene units. Moreover, alkylthiolation of 2-acetyl-5-bromothiophene with primary and tertiary thiols gave comparable yields (Scheme 4, CD35 and CD36) to the

Scheme 4. Expansion of Substrate Scope: Heteroaromatics^a

^a**Nickel:** Aryl halide (1 mmol), thiol (1.5 mmol), KOH (1.5 mmol), 1,4-dioxane (5 mL), 1 mol % of complex Ni B-1 for 6 h at 40 °C. **Palladium:** Aryl halide (1 mmol), thiol (1.5 mmol), NaOH (1.5 mmol), H₂O (5 mL), 1.5 mL of complex Pd B-1 for 4 h at 60 °C. Isolated yields from column chromatography.

products from unsubstituted bromothiophenes and bromothiazole (Scheme 4, CD26–CD34). Moreover, a heteroaryl ring possessing an *ortho*-substituted hydroxyl group was successfully coupled with 1-decanethiol (Scheme 4, CD37).

Having demonstrated C–S coupling from alkyl thiols, we also extended the scope of these catalysts by introducing 4-pyridine thiol for attaching a heteroaryl ring with *para*-substituted aryl bromide containing a hydroxy, acetyl, nitro, and nitrile functionality (Scheme 4, CD38–CD41). Introducing a heteroaryl moiety in the presence of these reactive groups, Ni B-1 and Pd B-1 maintained good to excellent yields. Wang et al. have reported an electrochemical system for synthesizing CD41 (Scheme 4) by *in situ* production of the catalyst in glovebox settings.¹⁸ In contrast, well-defined Ni B-1 and Pd B-1 catalytic systems have afforded excellent yields in aerobic reaction settings. Moreover, the need for harsh reaction conditions profoundly limits the C–S coupling of alkyl and heteroaryl thiols for generating medicinally important heteroaryl compounds.^{14,20,32,33} However, Ni B-1 and Pd B-1 manifested promising performance in milder reaction settings.

CONCLUSION

We have demonstrated air- and moisture-stable well-defined α -diimine Ni(II) and Pd(II) complexes for C–S cross-coupling. Versatile features of the α -diimine environment were examined by synthesizing four mononuclear and bridged dinuclear

complexes from iminopyridine- and acenaphthene-based ligand cores. Further, topographic steric maps and percent buried volume of the complexes were generated for understanding the shift in the steric characteristics. Steric attributes associated with the coordination nature were analyzed and correlated with the catalytic performance in Ni- and Pd-based systems. Prominently, the highest steric bulk associated with the bridged dinuclear Ni **B-1** afforded nearly quantitative yields in the cross-coupling of alkyl, heteroaryl thiols with aryl and heteroaryl bromides. Accordingly, Ni-based systems within α -diimine frameworks can be more sustainable and economical substitutes for Pd analogues to synthesize pharmaceutically active building blocks by C–S cross-coupling reactions.

EXPERIMENTAL SECTION

General Materials and Methods. All the chemicals were purchased from Fisher Scientific or Sigma-Aldrich and applied without further purification unless described. The ^1H NMR and ^{13}C NMR spectra were obtained by operating a 500 MHz Bruker AVANCE III spectrometer, using chloroform as the reference solvent. Elemental analysis of the synthesized α -diimine complexes was achieved through a Thermo FLASH 2000 CHN elemental analyzer. A Waters ACQUITY UPLC M-Class was applied for collecting the ESI-MS data. SambVca 2.1, a free web tool, was employed to generate the topographic steric maps and percent buried volume ($\%V_{\text{bur}}$) of the α -diimine complexes. All the reactions except for the synthesis of the α -diimine complexes were performed in air. As the thiols have an offensive smell, proper work practices were followed.

Single-Crystal XRD Data Characterization. For collecting the single-crystal X-ray diffraction data, an Incoatec microfocus Mo $K\alpha$ radiation source ($\lambda = 0.71073 \text{ \AA}$) was applied within a Bruker Kappa D8 Quest CPAD diffractometer. For the measurements, a Photon 100 CMOS detector was used, including an Oxford Cryosystems cooler. Data reduction and cell refinement were achieved through the Bruker SAINT and Bruker APEX3 graphical interface. The space groups' estimation and multiscan absorption correction were implemented using Bruker XPREP and SADABS, respectively. SHELXTL (intrinsic phasing method)⁴⁸ and SHELXL2017⁴⁹ were used for solving and refining the structure sequentially. Ultimately, ORTEP-3 was used for molecular graphics and publCIF software for obtaining the crystallographic information file (CIF).

Steric Map and Percent Buried Volume. For generating the steric maps and the percent buried volumes ($\%V_{\text{bur}}$), SambVca 2.1⁴⁰ was applied through <https://www.molnac.unisa.it/OMtools/sambvca2.1/index.html>. For this purpose, CIF or converted XYZ files of the complexes were used, including the radius of the sphere as 3.5 \AA , bond radii scaled by 1.17, and a mesh of 0.1 \AA .

Synthesis of Iminopyridine Ligand *N*-(4-Butylphenyl)-1-(pyridin-2-yl)methanimine (1a**).** The iminopyridine ligand **1a** was synthesized by following a reported procedure.³⁴ A one-neck 100 mL flask was charged with 2-pyridinecarboxaldehyde (3 mL, 0.032 mol), 4-butylaniline (5.05 mL, 0.032 mol), DMF (40 mL), and anhydrous MgSO_4 (120 mg, 1 mmol). After stirring the reaction mixture for 12 h at room temperature, three extractions were performed with ethyl acetate (40 mL) and distilled water (40 mL). The ethyl acetate layer was dried with anhydrous MgSO_4 . The crude product from the rotary evaporation was purified by employing *n*-hexane as an eluent through silica gel column chromatography. The pure product was isolated as a yellow oil (Yield = 5.98 g, 78.65%). ESI-MS m/z $[\text{M} + \text{H}]^+ = 239.0083$ (calculated for $\text{C}_{16}\text{H}_{18}\text{N}_2 = 239.0054$). ^1H NMR (500 MHz, CDCl_3 , 300 K), δ (ppm): 8.69 (d, $J = 4.70 \text{ Hz}$, 1H), 8.64 (s, 1H), 8.19 (d, $J = 7.90 \text{ Hz}$, 1H), 7.76 (t, $J = 7.80 \text{ Hz}$, 1H), 7.31 (q, $J = 5.65 \text{ Hz}$, 1H), 7.23 (q, $J = 8.05 \text{ Hz}$, 4H), 2.63 (t, $J = 7.70 \text{ Hz}$, 2H), 1.62 (q, $J = 7.55 \text{ Hz}$, 2H), 1.33–1.41 (m, 2H), 0.94 (t, $J = 7.4 \text{ Hz}$, 3H).

Synthesis of Iminopyridine Ligand *N*-(4-Isopropylphenyl)-1-(pyridin-2-yl)methanimine (1b**).** The iminopyridine ligand **1b** was synthesized by employing the above procedure using 2-

pyridinecarboxaldehyde (3 mL, 0.032 mol), and 4-isopropylaniline (4.4 mL, 0.032 mol). The pure product was isolated as a light yellow oil (Yield = 5.66 g, 78.81%). ESI-MS m/z $[\text{M} + \text{H}]^+ = 225.0013$ (calculated for $\text{C}_{15}\text{H}_{16}\text{N}_2 = 225.0097$). ^1H NMR (500 MHz, CDCl_3 , 300 K), δ (ppm): 8.70 (d, $J = 4.65 \text{ Hz}$, 1H), 8.62 (s, 1H), 8.20 (d, $J = 7.90 \text{ Hz}$, 1H), 7.79 (t, $J = 7.65 \text{ Hz}$, 1H), 7.34 (t, $J = 5.65 \text{ Hz}$, 1H), 7.25 (br, 4H), 2.94 (br, 1H), 1.27 (br, 6H). ^1H NMR data are consistent with the reported literature.⁵⁰

Synthesis of Iminopyridine Ligand *N*-(2-Isopropylphenyl)-1-(pyridin-2-yl)methanimine (1d**).** The iminopyridine ligand **1d** was synthesized by employing the above procedure using 2-pyridinecarboxaldehyde (3 mL, 0.032 mol), and 2-isopropylaniline (4.5 mL, 0.032 mol). The pure product was isolated as a light orange oil (Yield = 6.29 g, 87.67%). ESI-MS m/z $[\text{M} + \text{H}]^+ = 225.0057$ (calculated for $\text{C}_{15}\text{H}_{16}\text{N}_2 = 225.0074$). ^1H NMR (500 MHz, CDCl_3 , 300 K), δ (ppm): 8.71 (d, $J = 4.60 \text{ Hz}$, 1H), 8.53 (s, 1H), 8.26 (d, $J = 7.90 \text{ Hz}$, 1H), 7.82 (t, $J = 7.65 \text{ Hz}$, 1H), 7.33–7.38 (m, 2H), 7.21–7.25 (m, 2H), 7.00 (d, $J = 6.95 \text{ Hz}$, 1H), 3.52–3.60 (m, 1H), 1.26 (d, $J = 6.95 \text{ Hz}$, 6H). ^1H NMR data are consistent with the reported literature.⁵¹

Synthesis of the Acenaphthene Ligand *N*,*N*'-Bis(4-butylphenyl)acenaphthylene-1,2-diimine (1c**).** The acenaphthene ligand **1c** was synthesized by following a reported procedure.³⁴ A one-neck 100 mL flask was charged with acenaphthoquinone (1.71 g, 9.39 mmol), 4-butylaniline (2.87 g, 19.2 mmol), methanol (50 mL), and formic acid (1 mL). The reaction mixture was filtered after stirring for 10 h at room temperature. The isolated solid was washed with cold methanol (50 mL), followed by dissolving in dichloromethane. After filtering the solution through Celite, the pure product was obtained as an orange solid from slow evaporation (Yield = 2.98 g, 71.55%). ESI-MS m/z $[\text{M} + \text{H}]^+ = 445.0069$ (calculated for $\text{C}_{32}\text{H}_{32}\text{N}_2 = 445.0014$). ^1H NMR (500 MHz, CDCl_3 , 300 K), δ (ppm): 7.87 (d, $J = 8.2 \text{ Hz}$, 2H), 7.36 (t, $J = 7.60 \text{ Hz}$, 2H), 7.27 (d, $J = 7.90 \text{ Hz}$, 4H), 7.04 (d, $J = 8.20 \text{ Hz}$, 4H), 6.87 (d, $J = 7.25 \text{ Hz}$, 2H), 2.71 (t, $J = 7.7 \text{ Hz}$, 4H), 1.70 (q, $J = 7.40 \text{ Hz}$, 4H), 1.40–1.47 (m, 4H), 0.99 (t, $J = 7.35 \text{ Hz}$, 6H). ^{13}C NMR (500 MHz, CDCl_3 , 300 K), δ (ppm): 161.41, 149.53, 141.73, 139.06, 132.69, 131.25, 128.84, 128.76, 127.62, 123.89, 118.23, 35.30, 33.81, 22.49, 14.12.

Synthesis of the Iminopyridine Bis-Ligated Nickel(II) Complex (Ni A-1**).** Complex **Ni A-1** was synthesized by following a reported procedure.³⁴ A one-neck 50 mL flask was charged with dichloro-(dimethoxyethane)nickel(II) $\text{NiCl}_2(\text{DME})$ (219.72 mg, 1 mmol) with a magnetic stirrer. The flask was purged with nitrogen gas before adding the ligand **1a** (525 mg, 2 mmol) dissolved in dichloromethane (15 mL). The reaction mixture was filtered after stirring for 24 h at room temperature under a nitrogen atmosphere. The precipitated solid was washed with hexane (40 mL) and diethyl ether (40 mL). After drying for 24 h in vacuum, the pure product was isolated as a green solid (Yield = 474.21 mg, 78.22%). Elemental analysis: calculated for $\text{C}_{32}\text{H}_{36}\text{Cl}_2\text{N}_4\text{Ni}$: C, 63.40; H, 5.99; N, 9.24. Found: C, 63.30; H, 6.06; N, 9.17. Methanol solvent was used to make a saturated solution of the complex. After slow evaporation at room temperature, a suitable single crystal was obtained for single-crystal XRD analysis. Crystal size: $0.50 \times 0.25 \times 0.07 \text{ mm}^3$; crystal color: yellow; crystal shape: tablet.

Synthesis of the Iminopyridine Palladium(II) Complex (Pd A-1**).** Complex **Pd A-1** was synthesized by following a reported procedure.³⁴ A one-neck 50 mL flask was charged with ligand **1b** (166.83 mg, 0.70 mmol), dichloro(1,5-cyclooctadiene)palladium(II) known as $\text{PdCl}_2(\text{cod})$ (200 mg, 0.7 mmol) and a magnetic stirrer. The flask was purged with nitrogen gas before adding dichloromethane (15 mL). The reaction mixture was filtered after stirring for 8 h at room temperature under a nitrogen atmosphere. The precipitated solid was washed with hexane (40 mL) and diethyl ether (40 mL). After drying for 24 h in vacuum, the pure product was isolated as a dark orange solid (Yield = 174.21 mg, 83.56%). Elemental analysis: calculated for $\text{C}_{15}\text{H}_{16}\text{Cl}_2\text{N}_2\text{Pd}$: C, 44.86; H, 4.02; N, 6.98. Found: C, 44.79; H, 4.09; N, 6.88. Dimethyl sulfoxide solvent was used to make a saturated solution of the complex. After slow evaporation at room temperature, a suitable single crystal was

obtained for single-crystal XRD analysis. Crystal size: $0.70 \times 0.64 \times 0.08$ mm³; crystal color: orange; crystal shape: plate.

Synthesis of the Acenaphthene Palladium(II) Complex (Pd B-1). Complex Pd B-1 was synthesized utilizing the aforementioned procedure from PdCl₂(cod) (200 mg, 0.7 mmol) and ligand 1c (311.23 mg, 0.70 mmol). The pure product was isolated as a dark orange solid (Yield = 421.21 mg, 87.28%). Elemental analysis: calculated for C₃₂H₃₂Cl₂N₂Pd: C, 61.80; H, 5.19; N, 4.50. Found: C, 61.71; H, 5.09; N, 4.63. Dimethyl sulfoxide solvent was used to make a saturated solution of the complex. After slow evaporation at room temperature, a suitable single crystal was obtained for single-crystal XRD analysis. Crystal size: $0.36 \times 0.34 \times 0.12$ mm³; crystal color: orange; crystal shape: tablet.

Synthesis of the Iminopyridine Monoligated Nickel(II) Complex (Ni B-1). Complex Ni B-1 was synthesized utilizing the procedure for Ni A-1 possessing ligand 1d (525 mg, 1 mmol) and dichloro-(dimethoxyethane)nickel(II) NiCl₂(DME) (219.72 mg, 1 mmol). The pure product was isolated as a dark green solid (Yield = 595.27 mg, 89.45%). Elemental analysis: calculated for C₃₀H₃₂Cl₄N₄Ni₂: C, 50.91; H, 4.56; N, 7.92. Found: C, 50.78; H, 4.41; N, 7.84. Methanol solvent was used to make a saturated solution of the complex. After slow evaporation at room temperature, a suitable single crystal was obtained for single-crystal XRD analysis. Crystal size: $0.54 \times 0.34 \times 0.16$ mm³; crystal color: green; crystal shape: fragment.

General Procedure for Nickel-Catalyzed C–S Cross-Coupling. A one-neck 25 mL flask was charged with thiol (1.5 mmol), aryl halide (1 mmol), KOH (1.5 mmol), 1,4-dioxane (5 mL), 1 mol % of complex Ni A-1 or Ni B-1, and a magnetic stirrer. After capping with a rubber septum, the reaction mixture was stirred for 6 h at 40 °C in air. Three extractions were carried out with water (20 mL) and ethyl acetate (20 mL). The crude product was collected after subsequent drying and concentrating the ethyl acetate layer. The pure product was isolated after silica gel (200–300 mesh) column chromatography purification.

General Procedure for Palladium-Catalyzed C–S Cross-Coupling. A two-neck 25 mL flask carrying a condenser was charged with thiol (1.5 mmol), aryl halide (1 mmol), NaOH (1.5 mmol), H₂O (5 mL), 1.5 mL of complex Pd A-1 or Pd B-1, and a magnetic stirrer. After capping with rubber septa, the reaction mixture was stirred for 4 h at 60 °C in air. Three extractions were carried out with water (20 mL) and ethyl acetate (20 mL). The crude product was collected after subsequent drying and concentrating the ethyl acetate layer. The pure product was isolated after silica gel (200–300 mesh) column chromatography purification.

Hexyl(naphthalen-2-yl)sulfane (CD1). Silica gel column chromatography having eluent as *n*-hexane. Colorless oil. Yield: 217.5 mg, 89% (Ni A-1); 237.1 mg, 97% (Ni B-1); 229.7 mg, 94% (Pd A-1); 232.1 mg, 95% (Pd B-1). ESI-MS m/z [M + H]⁺ = 245.0029 (calculated for C₁₆H₂₀S, 245.0047). ¹H NMR (500 MHz, CDCl₃, 300 K): δ (ppm): 7.81–7.75 (m, 4H), 7.50–7.42 (m, 3H), 3.04 (t, J = 7.39 Hz, 2H), 1.75–1.69 (m, 2H), 1.52–1.46 (m, 2H), 1.20 (s, 4H), 0.89 (t, J = 6.65 Hz, 3H). ¹³C NMR (500 MHz, CDCl₃, 300 K): δ (ppm): 134.80, 133.94, 131.74, 128.36, 127.81, 127.34, 127.09, 126.55, 126.42, 125.55, 33.63, 31.49, 29.20, 28.69, 22.66, 14.12. NMR data are consistent with the reported literature.³⁰

Decyl(naphthalen-2-yl)sulfane (CD2). Silica gel column chromatography having eluent as *n*-hexane. Colorless oil. Yield: 243.4 mg, 81% (Ni A-1); 294.4 mg, 98% (Ni B-1); 276.4 mg, 92% (Pd A-1); 285.4 mg, 95% (Pd B-1). ESI-MS m/z [M + H]⁺ = 301.0075 (calculated for C₂₀H₂₈S, 301.0147). ¹H NMR (500 MHz, CDCl₃, 300 K): δ (ppm): 7.773–7.832 (m, 4H), 7.448–7.525 (m, 3H), 3.058–3.087 (t, J = 7.47 Hz, 2H), 1.733–1.793 (m, 2H), 1.499–1.527 (m, 2H), 1.34 (12H), 0.97 (t, J = 6.56 Hz, 3H). ¹³C NMR (500 MHz, CDCl₃, 300 K): δ (ppm): 134.83, 133.93, 131.70, 128.32, 127.77, 127.27, 127.04, 126.52, 126.32, 125.47, 33.54, 32.01, 29.66, 29.63, 29.43, 29.29, 29.20, 28.99, 22.79, 14.23.

Hexyl(naphthalen-1-yl)sulfane (CD3). Silica gel column chromatography having eluent as *n*-hexane. Colorless oil. Yield: 212.6 mg, 87% (Ni A-1); 234.6 mg, 96% (Ni B-1); 212.6 mg, 87% (Pd A-1);

222.4 mg, 91% (Pd B-1). ESI-MS m/z [M + H]⁺ = 245.0021 (calculated for C₁₆H₂₀S, 245.00847). ¹H NMR (500 MHz, CDCl₃, 300 K): δ (ppm): 8.50 (d, J = 8.36 Hz, 1H), 7.89 (d, J = 8.02 Hz, 1H), 7.76 (d, J = 8.18 Hz, 1H), 7.63–7.60 (m, 2H), 7.55 (t, J = 7.80 Hz, 1H), 7.46 (t, J = 7.70 Hz, 1H), 3.04 (t, J = 7.35 Hz, 2H), 1.75–1.72 (m, 2H), 1.52–1.49 (m, 2H), 1.36 (s, 4H), 0.96 (t, J = 6.67 Hz, 3H). ¹³C NMR (500 MHz, CDCl₃, 300 K): δ (ppm): 134.39, 133.97, 132.95, 128.57, 127.40, 126.83, 126.26, 126.18, 125.59, 125.10, 34.26, 31.47, 29.20, 28.65, 22.62, 14.09. NMR data are consistent with the reported literature.³⁰

Decyl(naphthalen-1-yl)sulfane (CD4). Silica gel column chromatography having eluent as *n*-hexane. Colorless oil. Yield: 270.4 mg, 90% (Ni A-1); 288.4 mg, 96% (Ni B-1); 276.4 mg, 92% (Pd A-1); 285.4 mg, 95% (Pd B-1). ESI-MS m/z [M + H]⁺ = 301.0103 (calculated for C₂₀H₂₈S, 301.0089). ¹H NMR (500 MHz, CDCl₃, 300 K): δ (ppm): 8.49 (d, J = 8.41 Hz, 1H), 7.88 (d, J = 7.95 Hz, 1H), 7.75 (d, J = 8.2 Hz, 1H), 7.71–7.57 (m, 2H), 7.56 (t, J = 6.72 Hz, 1H), 7.45 (t, J = 7.75 Hz, 1H), 3.03 (t, J = 7.38 Hz, 2H), 1.76–1.70 (m, 2H), 1.55–1.49 (m, 2H), 1.32 (s, 12H), 0.97 (t, J = 6.99 Hz, 3H). ¹³C NMR (500 MHz, CDCl₃, 300 K): δ (ppm): 134.43, 134.01, 132.99, 128.61, 127.45, 126.86, 126.29, 126.22, 125.63, 125.14, 34.29, 32.02, 29.66, 29.63, 29.43, 29.32, 29.27, 29.02, 22.81, 14.23. NMR data are consistent with the reported literature.³⁰

Benzyl(naphthalen-2-yl)sulfane (CD5). Silica gel column chromatography having eluent as *n*-hexane. Yellow oil. Yield: 227.8 mg, 91% (Ni A-1); 245.3 mg, 98% (Ni B-1); 232.8 mg, 93% (Pd A-1); 240.3 mg, 96% (Pd B-1). ESI-MS m/z [M + H]⁺ = 251.0119 (calculated for C₁₇H₁₄S, 251.0128). ¹H NMR (500 MHz, CDCl₃, 300 K): δ (ppm): 7.88 (s, 1H), 7.83–7.77 (m, 2H), 7.72 (s, 1H), 7.70 (s, 1H), 7.48–7.40 (m, 4H), 7.34–7.22 (m, 3H), 4.22 (s, 2H). ¹³C NMR (500 MHz, CDCl₃, 300 K): δ (ppm): 137.51, 134.1, 132.47, 132.05, 128.99, 128.67, 127.85, 127.57, 127.36, 127.29, 126.76, 126.60, 126.35, 125.87, 39.09. NMR data are consistent with the reported literature.⁵²

4-(Phenylthio)pyridine (CD6). Silica gel column chromatography having eluent as *n*-hexane and ethyl acetate of 10:1 (v/v). Yellow solid. Yield: 146.0 mg, 78% (Ni A-1); 181.6 mg, 97% (Ni B-1); 155.4 mg, 83% (Pd A-1); 168.5 mg, 90% (Pd B-1). ESI-MS m/z [M + H]⁺ = 188.0013 (calculated for C₁₁H₉NS, 188.026). ¹H NMR (500 MHz, CDCl₃, 300 K): δ (ppm): 8.362 (2H), 7.448–7.547 (m, 5H), 6.941 (2H). ¹³C NMR (500 MHz, CDCl₃, 300 K): δ (ppm): 150.44, 149.50, 135.28, 130.02, 129.77, 129.55, 121.00. NMR data are consistent with the reported literature.⁵³

4-(Naphthalen-2-ylthio)pyridine (CD7). Silica gel column chromatography having eluent as *n*-hexane and ethyl acetate of 10:1 (v/v). Yellow solid. Yield: 170.8 mg, 72% (Ni A-1); 232.5 mg, 98% (Ni B-1); 163.7 mg, 69% (Pd A-1); 215.9 mg, 91% (Pd B-1). ESI-MS m/z [M + H]⁺ = 238.0128 (calculated for C₁₅H₁₁NS, 238.0113). ¹H NMR (500 MHz, CDCl₃, 300 K): δ (ppm): 8.339 (s, 2H), 8.106 (s, 1H), 7.835–7.907 (m, 3H), 7.520–7.589 (m, 3H), 6.979 (s, 2H). ¹³C NMR (500 MHz, CDCl₃, 300 K): δ (ppm): 150.46, 149.49, 135.21, 134.03, 133.53, 131.25, 129.86, 128.02, 128.00, 127.59, 127.12, 126.78, 121.17. NMR data are consistent with the reported literature.⁵⁴

4-(Naphthalen-1-ylthio)pyridine (CD8). Silica gel column chromatography having eluent as *n*-hexane and ethyl acetate of 10:1 (v/v). Dark yellow solid. Yield: 180.3 mg, 76% (Ni A-1); 220.7 mg, 93% (Ni B-1); 199.3 mg, 84% (Pd A-1); 211.2 mg, 89% (Pd B-1). ESI-MS m/z [M + H]⁺ = 238.0102 (calculated for C₁₅H₁₁NS, 238.0113). ¹H NMR (500 MHz, CDCl₃, 300 K): δ (ppm): 8.25 (m, 3H), 7.98 (d, J = 8.25 Hz, 1H), 7.90 (d, J = 7.45 Hz, 1H), 7.76 (d, J = 6.92 Hz, 1H), 7.52 (m, 3H), 6.80 (d, J = 6.25 Hz, 2H). ¹³C NMR (500 MHz, CDCl₃, 300 K): δ (ppm): 150.14, 149.33, 135.92, 134.46, 134.34, 131.41, 128.85, 127.72, 126.85, 126.08, 125.99, 125.62, 120.48.

2-Methyl-5-(tritylthio)pyrimidine (CD9). Silica gel column chromatography having eluent as *n*-hexane and ethyl acetate of 10:1 (v/v). Dark yellow solid. Yield: 232.1 mg, 63% (Ni A-1); 350.0 mg, 95% (Ni B-1); 257.9 mg, 70% (Pd A-1); 331.6 mg, 90% (Pd B-1). ESI-MS m/z [M + H]⁺ = 369.0183 (calculated for C₂₄H₂₀N₂S, 369.0155). ¹H NMR (500 MHz, CDCl₃, 300 K): δ (ppm): 8.35 (s, 2H), 7.00–7.10

(m, 9H), 6.88 (d, $J = 6.0$ Hz, 6H), 2.50 (s, 3H). ^{13}C NMR (500 MHz, CDCl_3 , 300 K), δ (ppm): 158.47, 144.58, 143.34, 131.75, 130.88, 129.47, 128.59, 126.70, 56.54.

4-(Hexylthio)phenol (CD10). Silica gel column chromatography having eluent as *n*-hexane and ethyl acetate of 10:1 (v/v). White solid. Yield: 204.0 mg, 97% (Ni B-1); 191.4 mg, 91% (Pd B-1). ESI-MS m/z $[\text{M} + \text{H}]^+ = 211.0015$ (calculated for $\text{C}_{12}\text{H}_{18}\text{OS}$, 211.0034). ^1H NMR (500 MHz, CDCl_3 , 300 K): δ (ppm): 7.28 (d, $J = 8.50$ Hz, 2H), 6.77 (d, $J = 8.50$ Hz, 2H), 5.28 (s, 1H), 2.80 (t, $J = 7.39$ Hz, 2H), 1.60–1.54 (m, 2H), 1.41–1.36 (m, 2H), 1.29–1.25 (m, 4H), 0.89 (t, $J = 6.90$ Hz, 3H). ^{13}C NMR (500 MHz, CDCl_3 , 300 K), δ (ppm): 153.93, 133.26, 127.17, 116.13, 36.01, 31.51, 29.43, 28.51, 22.66, 14.13.

4-(Decylthio)phenol (CD11). Silica gel column chromatography having eluent as *n*-hexane and ethyl acetate of 10:1 (v/v). White solid. Yield: 255.7 mg, 96% (Ni B-1); 247.7 mg, 93% (Pd B-1). ESI-MS m/z $[\text{M} + \text{H}]^+ = 267.0126$ (calculated for $\text{C}_{16}\text{H}_{26}\text{OS}$, 267.0076). ^1H NMR (500 MHz, CDCl_3 , 300 K): δ (ppm): 7.28 (d, $J = 8.27$ Hz, 2H), 6.77 (d, $J = 8.28$ Hz, 2H), 5.38 (s, 1H), 2.80 (t, $J = 7.32$ Hz, 2H), 1.58–1.54 (m, 2H), 1.37 (br, 2H), 1.25 (br, 12H), 0.87 (t, $J = 6.45$ Hz, 3H). ^{13}C NMR (500 MHz, CDCl_3 , 300 K), δ (ppm): 154.99, 133.27, 127.15, 116.12, 36.02, 32.02, 29.67, 29.65, 29.48, 29.43, 29.31, 28.85, 22.81, 14.23.

4-(Benzylthio)phenol (CD12). Silica gel column chromatography having eluent as *n*-hexane and ethyl acetate of 20:1 (v/v). White solid. Yield: 211.9 mg, 98% (Ni B-1); 196.8 mg, 91% (Pd B-1). ESI-MS m/z $[\text{M} + \text{H}]^+ = 217.0103$ (calculated for $\text{C}_{13}\text{H}_{12}\text{OS}$, 217.0018). ^1H NMR (500 MHz, CDCl_3 , 300 K): δ (ppm): 7.07–7.17 (m, 7H), 6.61–6.63 (m, 2H), 4.90 (br, 1H), 3.89 (s, 2H). ^{13}C NMR (500 MHz, CDCl_3 , 300 K), δ (ppm): 155.44, 138.17, 134.48, 129.01, 128.48, 127.11, 126.18, 116.06, 41.37. NMR data are consistent with the reported literature.⁵⁵

4-(Tritylthio)phenol (CD13). Silica gel column chromatography having eluent as *n*-hexane and ethyl acetate of 30:1 (v/v). White solid. Yield: 364.8 mg, 99% (Ni B-1); 350.0 mg, 95% (Pd B-1). ESI-MS m/z $[\text{M} + \text{H}]^+ = 369.0063$ (calculated for $\text{C}_{25}\text{H}_{20}\text{OS}$, 369.0071). ^1H NMR (500 MHz, CDCl_3 , 300 K): δ (ppm): 7.80–7.82 (m, 4H), 7.59 (t, $J = 7.4$ Hz, 2H), 7.49 (t, $J = 7.8$ Hz, 4H), 7.28 (t, $J = 7.2$ Hz, 4H), 7.21 (m, 3H), 7.11–7.13 (m, 3H). ^{13}C NMR (500 MHz, CDCl_3 , 300 K), δ (ppm): 144.05, 137.78, 132.55, 131.33, 130.20, 129.60, 128.42, 127.53, 126.43.

4-(tert-Butylthio)phenol (CD14). Silica gel column chromatography having eluent as *n*-hexane and ethyl acetate of 10:1 (v/v). White solid. Yield: 174.9 mg, 96% (Ni B-1); 169.5 mg, 93% (Pd B-1). ESI-MS m/z $[\text{M} + \text{H}]^+ = 183.0169$ (calculated for $\text{C}_{10}\text{H}_{14}\text{OS}$, 183.0146). ^1H NMR (500 MHz, CDCl_3 , 300 K): δ (ppm): 7.39 (d, $J = 8.58$ Hz, 2H), 6.80 (d, $J = 8.59$ Hz, 2H), 5.762 (br, 1H), 1.26 (s, 9H). ^{13}C NMR (500 MHz, CDCl_3 , 300 K), δ (ppm): 156.52, 139.18, 123.58, 115.72, 45.83, 30.81. NMR data are consistent with the reported literature.¹²

1-(4-(tert-Butylthio)phenyl)ethan-1-one (CD15). Silica gel column chromatography having eluent as *n*-hexane and ethyl acetate of 20:1 (v/v). Brown solid. Yield: 204.1 mg, 98% (Ni B-1); 187.4 mg, 90% (Pd B-1). ESI-MS m/z $[\text{M} + \text{H}]^+ = 209.0254$ (calculated for $\text{C}_{12}\text{H}_{16}\text{OS}$, 209.0187). ^1H NMR (500 MHz, CDCl_3 , 300 K): δ (ppm): 7.89 (d, $J = 8.24$ Hz, 2H), 7.60 (d, $J = 8.23$ Hz, 2H), 2.60 (s, 3H), 1.32 (s, 9H). ^{13}C NMR (500 MHz, CDCl_3 , 300 K), δ (ppm): 197.82, 139.56, 137.00, 136.92, 128.31, 47.01, 31.24, 26.78. NMR data are consistent with the reported literature.²⁶

1-(4-(Hexylthio)phenyl)ethan-1-one (CD16). Silica gel column chromatography having eluent as *n*-hexane and ethyl acetate of 10:1 (v/v). Brown solid. Yield: 289.5 mg, 99% (Ni B-1); 272.0 mg, 93% (Pd B-1). ESI-MS m/z $[\text{M} + \text{H}]^+ = 237.0033$ (calculated for $\text{C}_{14}\text{H}_{20}\text{OS}$, 237.0067). ^1H NMR (500 MHz, CDCl_3 , 300 K): δ (ppm): 7.85 (d, $J = 8.44$ Hz, 2H), 7.29 (d, $J = 8.48$ Hz, 2H), 3.00 (t, $J = 7.40$ Hz, 2H), 2.57 (s, 3H), 1.73–1.67 (m, 2H), 1.49–1.43 (m, 2H), 1.32 (br, 4H), 0.90 (t, $J = 6.73$ Hz, 3H). ^{13}C NMR (500 MHz, CDCl_3 , 300 K), δ (ppm): 197.03, 145.04, 133.71, 128.72, 126.23, 31.97, 31.33, 28.72, 28.57, 26.36, 22.52, 14.00. NMR data are consistent with the reported literature.³²

1-(4-(Decylthio)phenyl)ethan-1-one (CD17). Silica gel column chromatography having eluent as *n*-hexane and ethyl acetate of 10:1 (v/v). White solid. Yield: 274.9 mg, 94% (Ni B-1); 269.0 mg, 92% (Pd B-1). ESI-MS m/z $[\text{M} + \text{H}]^+ = 293.0167$ (calculated for $\text{C}_{18}\text{H}_{28}\text{OS}$, 293.0172). ^1H NMR (500 MHz, CDCl_3 , 300 K): δ (ppm): 7.84 (d, $J = 8.46$ Hz, 2H), 7.29 (d, $J = 8.47$ Hz, 2H), 2.98 (t, $J = 7.41$ Hz, 2H), 2.56 (s, 3H), 1.72–1.66 (m, 2H), 1.47–1.41 (m, 2H), 1.26 (s, 12H), 0.88 (t, $J = 6.83$ Hz, 3H). ^{13}C NMR (500 MHz, CDCl_3 , 300 K), δ (ppm): 197.30, 145.16, 133.86, 128.87, 126.40, 32.12, 32.01, 29.65, 29.61, 29.42, 29.27, 29.03, 28.88, 26.54, 22.80, 14.23.

tert-Butyl(4-nitrophenyl)sulfane (CD18). Silica gel column chromatography having eluent as *n*-hexane and ethyl acetate of 20:1 (v/v). White solid. Yield: 202.8 mg, 96% (Ni B-1); 204.9 mg, 97% (Pd B-1). ESI-MS m/z $[\text{M} + \text{H}]^+ = 212.0102$ (calculated for $\text{C}_{10}\text{H}_{13}\text{NO}_2\text{S}$, 212.0197). ^1H NMR (500 MHz, CDCl_3 , 300 K): δ (ppm): 7.21 (d, $J = 8.49$ Hz, 2H), 6.53 (d, $J = 8.50$ Hz, 2H), 1.17 (s, 9H). ^{13}C NMR (500 MHz, CDCl_3 , 300 K), δ (ppm): 147.23, 138.87, 120.69, 114.99, 45.40, 30.80. NMR data are consistent with the reported literature.⁵⁶

Hexyl(4-nitrophenyl)sulfane (CD19). Silica gel column chromatography having eluent as *n*-hexane and ethyl acetate of 10:1 (v/v). White solid. Yield: 234.5 mg, 98% (Ni B-1); 229.7 mg, 96% (Pd B-1). ESI-MS m/z $[\text{M} + \text{H}]^+ = 240.0063$ (calculated for $\text{C}_{12}\text{H}_{17}\text{NO}_2\text{S}$, 240.0017). ^1H NMR (500 MHz, CDCl_3 , 300 K): δ (ppm): 7.51 (d, $J = 8.34$ Hz, 2H), 6.85 (d, $J = 8.29$ Hz, 2H), 3.05 (t, $J = 7.41$ Hz, 2H), 1.87–1.82 (m, 2H), 1.68–1.65 (m, 2H), 1.58–1.54 (m, 4H), 1.16 (t, $J = 6.96$ Hz, 3H). ^{13}C NMR (500 MHz, CDCl_3 , 300 K), δ (ppm): 145.64, 133.66, 124.03, 115.73, 36.50, 31.47, 29.45, 28.45, 22.61, 14.09. NMR data are consistent with the reported literature.⁵⁷

Decyl(4-nitrophenyl)sulfane (CD20). Silica gel column chromatography having eluent as *n*-hexane and ethyl acetate of 10:1 (v/v). White solid. Yield: 280.6 mg, 95% (Ni B-1); 280.6 mg, 95% (Pd B-1). ESI-MS m/z $[\text{M} + \text{H}]^+ = 296.0028$ (calculated for $\text{C}_{16}\text{H}_{23}\text{NO}_2\text{S}$, 296.0046). ^1H NMR (500 MHz, CDCl_3 , 300 K): δ (ppm): 7.27 (d, $J = 7.16$ Hz, 2H), 6.66 (d, $J = 7.09$ Hz, 2H), 2.80 (t, $J = 6.84$ Hz, 2H), 1.60–1.58 (m, 2H), 1.41 (br, 2H), 1.29 (br, 12H), 0.92 (t, $J = 6.68$ Hz, 3H). ^{13}C NMR (500 MHz, CDCl_3 , 300 K), δ (ppm): 145.47, 133.80, 129.32, 115.70, 36.54, 32.02, 29.67, 29.54, 29.43, 29.32, 28.85, 22.80, 14.24.

Benzyl(4-nitrophenyl)sulfane (CD21). Silica gel column chromatography having eluent as *n*-hexane and ethyl acetate of 20:1 (v/v). White solid. Yield: 237.9 mg, 97% (Ni B-1); 223.2 mg, 91% (Pd B-1). ESI-MS m/z $[\text{M} + \text{H}]^+ = 246.0215$ (calculated for $\text{C}_{13}\text{H}_{11}\text{NO}_2\text{S}$, 246.00138). ^1H NMR (500 MHz, CDCl_3 , 300 K): δ (ppm): 7.29–7.15 (m, 7H), 6.58 (d, $J = 7.56$ Hz, 2H), 3.97 (s, 2H). ^{13}C NMR (500 MHz, CDCl_3 , 300 K), δ (ppm): 146.22, 138.57, 134.80, 129.05, 126.94, 123.22, 115.64, 41.92. NMR data are consistent with the reported literature.⁵⁸

4-(tert-Butylthio)-2,6-difluorobenzonitrile (CD22). Silica gel column chromatography having eluent as *n*-hexane and ethyl acetate of 10:1 (v/v). White solid. Yield: 215.9 mg, 95% (Ni B-1); 209.1 mg, 92% (Pd B-1). ESI-MS m/z $[\text{M} + \text{H}]^+ = 228.0192$ (calculated for $\text{C}_{11}\text{H}_{11}\text{F}_2\text{NS}$, 228.0075). ^1H NMR (500 MHz, CDCl_3 , 300 K): δ (ppm): 7.78 (s, 2H), 1.32 (s, 9H). ^{13}C NMR (500 MHz, CDCl_3 , 300 K), δ (ppm): 146.39, 138.21, 138.12, 129.09, 117.20, 49.74, 31.19.

4-(tert-Butylthio)benzonitrile (CD23). Silica gel column chromatography having eluent as *n*-hexane and ethyl acetate of 30:1 (v/v). White solid. Yield: 187.4 mg, 98% (Ni B-1); 177.8 mg, 93% (Pd B-1). ESI-MS m/z $[\text{M} + \text{H}]^+ = 192.0351$ (calculated for $\text{C}_{11}\text{H}_{13}\text{NS}$, 192.0187). ^1H NMR (500 MHz, CDCl_3 , 300 K): δ (ppm): 7.57–7.61 (m, 4H), 1.30 (s, 9H). ^{13}C NMR (500 MHz, CDCl_3 , 300 K), δ (ppm): 139.87, 137.18, 131.94, 118.57, 112.18, 47.35, 31.13. NMR data are consistent with the reported literature.⁵⁹

4-(Decylthio)-2,6-difluorobenzonitrile (CD24). Silica gel column chromatography having eluent as *n*-hexane and ethyl acetate of 30:1 (v/v). White solid. Yield: 295.8 mg, 95% (Ni B-1); 277.1 mg, 89% (Pd B-1). ESI-MS m/z $[\text{M} + \text{H}]^+ = 312.0217$ (calculated for $\text{C}_{17}\text{H}_{23}\text{F}_2\text{NS}$, 312.0146). ^1H NMR (500 MHz, CDCl_3 , 300 K): δ (ppm): 7.30 (s, 1H), 7.23 (s, 1H), 3.03 (t, $J = 7.01$ Hz, 2H), 1.76–

1.73 (m, 2H), 1.32 (s, 14H), 0.92 (t, J = 6.43 Hz, 3H). ^{13}C NMR (500 MHz, CDCl_3 , 300 K), δ (ppm): 146.29, 127.73, 126.30, 114.78, 110.37, 33.31, 32.02, 29.65, 29.57, 29.42, 29.21, 28.89, 28.55, 22.81, 14.24.

4-(Decylthio)benzonitrile (CD25). Silica gel column chromatography having eluent as *n*-hexane and ethyl acetate of 10:1 (v/v). White solid. Yield: 256.1 mg, 93% (**Ni B-1**); 247.9 mg, 90% (**Pd B-1**). ESI-MS m/z $[\text{M} + \text{H}]^+ = 276.0078$ (calculated for $\text{C}_{17}\text{H}_{25}\text{NS}$, 276.0043). ^1H NMR (500 MHz, CDCl_3 , 300 K): δ (ppm): 7.51 (d, J = 8.41 Hz, 2H), 7.28 (d, J = 8.41 Hz, 2H), 2.96 (t, J = 7.40 Hz, 2H), 1.66–1.72 (m, 2H), 1.41–1.47 (m, 2H), 1.261 (b, 12H), 0.88 (t, J = 6.91 Hz, 3H). ^{13}C NMR (500 MHz, CDCl_3 , 300 K), δ (ppm): 145.48, 132.32, 126.82, 119.09, 108.06, 32.07, 32.01, 29.64, 29.59, 29.41, 29.24, 29.00, 28.71, 22.80, 14.23.

3-(tert-Butylthio)thiophene (CD26). Silica gel column chromatography having eluent as *n*-hexane and ethyl acetate of 30:1 (v/v). Colorless oil. Yield: 165.4 mg, 96% (**Ni B-1**); 163.6 mg, 95% (**Pd B-1**). ESI-MS m/z $[\text{M} + \text{H}]^+ = 173.0032$ (calculated for $\text{C}_8\text{H}_{12}\text{S}_2$, 173.0077). ^1H NMR (500 MHz, CDCl_3 , 300 K): δ (ppm): 7.43 (d, 1H), 7.31 (m, 1H), 7.10 (d, 1H), 1.31 (s, 9H). ^{13}C NMR (500 MHz, CDCl_3 , 300 K), δ (ppm): 134.51, 131.98, 129.22, 125.30, 45.96, 31.05.

3-(Hexylthio)thiophene (CD27). Silica gel column chromatography having eluent as *n*-hexane and ethyl acetate of 30:1 (v/v). Colorless oil. Yield: 196.3 mg, 98% (**Ni B-1**); 182.3 mg, 91% (**Pd B-1**). ESI-MS m/z $[\text{M} + \text{H}]^+ = 201.0032$ (calculated for $\text{C}_{10}\text{H}_{16}\text{S}_2$, 201.0077). ^1H NMR (500 MHz, CDCl_3 , 300 K): δ (ppm): 7.30 (dd, J = 7.96 Hz, J = 4.96 Hz, 1H), 7.10 (d, J = 7.95 Hz, 1H), 7.01 (d, J = 4.95 Hz, 1H), 2.84 (t, J = 7.62 Hz, 2H), 1.57–1.61 (m, 2H), 1.37–1.40 (m, 2H), 1.26–1.31 (m, 4H), 0.87–0.90 (m, 3H). ^{13}C NMR (500 MHz, CDCl_3 , 300 K), δ (ppm): 132.49, 129.78, 126.09, 122.99, 35.47, 31.49, 29.50, 28.51, 22.69, 14.12. NMR data are consistent with the reported literature.⁶⁰

3-(Decylthio)thiophene (CD28). Silica gel column chromatography having eluent as *n*-hexane and ethyl acetate of 30:1 (v/v). Colorless oil. Yield: 253.9 mg, 99% (**Ni B-1**); 238.5 mg, 93% (**Pd B-1**). ESI-MS m/z $[\text{M} + \text{H}]^+ = 257.0068$ (calculated for $\text{C}_{18}\text{H}_{26}\text{S}_2$, 257.0057). ^1H NMR (500 MHz, CDCl_3 , 300 K): δ (ppm): 7.31 (d, J = 2.89 Hz, 1H), 7.12 (d, J = 2.69 Hz, 1H), 7.02 (d, J = 4.92 Hz, 1H), 2.85 (t, J = 7.28 Hz, 2H), 1.64–1.61 (m, 2H), 1.29 (s, 14H), 0.90 (t, J = 6.82 Hz, 3H). ^{13}C NMR (500 MHz, CDCl_3 , 300 K), δ (ppm): 132.51, 129.73, 126.03, 122.90, 35.43, 32.00, 29.65, 29.62, 29.51, 29.41, 29.28, 28.82, 22.79, 14.21. NMR data are consistent with the reported literature.⁶¹

2-(tert-Butylthio)thiophene (CD29). Silica gel column chromatography having eluent as *n*-hexane and ethyl acetate of 30:1 (v/v). Colorless oil. Yield: 167.1 mg, 97% (**Ni B-1**); 155.0 mg, 90% (**Pd B-1**). ESI-MS m/z $[\text{M} + \text{H}]^+ = 173.0029$ (calculated for $\text{C}_8\text{H}_{12}\text{S}_2$, 173.0077). ^1H NMR (500 MHz, CDCl_3 , 300 K): δ (ppm): 7.41 (d, J = 5.37 Hz, 1H), 7.14 (d, J = 3.50 Hz, 1H), 7.02–7.04 (dd, J = 5.36 Hz, J = Hz, 3.49, 1H), 1.31 (s, 9H). ^{13}C NMR (500 MHz, CDCl_3 , 300 K), δ (ppm): 137.02, 132.02, 130.83, 127.60, 46.84, 30.67.

2-(Hexylthio)thiophene (CD30). Silica gel column chromatography having eluent as *n*-hexane and ethyl acetate of 30:1 (v/v). Colorless oil. Yield: 196.3 mg, 98% (**Ni B-1**); 192.3 mg, 96% (**Pd B-1**). ESI-MS m/z $[\text{M} + \text{H}]^+ = 201.0051$ (calculated for $\text{C}_{10}\text{H}_{16}\text{S}_2$, 201.0077). ^1H NMR (500 MHz, CDCl_3 , 300 K): δ (ppm): 7.30 (dd, J = 5.35, 1.10 Hz, 1H), 7.11 (dd, J = 3.55, 1.10 Hz, 1H), 6.97 (dd, J = 5.25, 3.62 Hz, 1H), 2.80 (t, J = 7.07 Hz, 2H), 1.65–1.56 (m, 2H), 1.44–1.38 (m, 2H), 1.33–1.28 (m, 4H), 0.91 (t, J = 6.99 Hz, 3H). ^{13}C NMR (500 MHz, CDCl_3 , 300 K), δ (ppm): 135.16, 133.21, 128.87, 127.47, 39.05, 31.44, 29.45, 28.19, 22.62, 14.10. NMR data are consistent with the reported literature.⁶⁰

2-(Decylthio)thiophene (CD31). Silica gel column chromatography having eluent as *n*-hexane and ethyl acetate of 30:1 (v/v). Colorless oil. Yield: 238.5 mg, 93% (**Ni B-1**); 233.3 mg, 91% (**Pd B-1**). ESI-MS m/z $[\text{M} + \text{H}]^+ = 257.0093$ (calculated for $\text{C}_{18}\text{H}_{26}\text{S}_2$, 257.0057). ^1H NMR (500 MHz, CDCl_3 , 300 K): δ (ppm): 7.32 (dd, J = 5.33, 0.86 Hz, 1H), 7.11 (dd, J = 3.45, 0.91 Hz, 1H), 6.96 (dd, J = 5.30, 3.55 Hz, 1H), 2.80 (t, J = 7.37 Hz, 2H), 1.65–1.59 (m, 2H),

1.42–1.39 (m, 2H), 1.28 (s, 12H), 0.90 (t, J = 6.89 Hz, 3H). ^{13}C NMR (500 MHz, CDCl_3 , 300 K), δ (ppm): 135.21, 133.20, 128.86, 127.46, 39.07, 32.01, 29.65, 29.62, 29.51, 29.42, 29.26, 28.54, 22.79, 14.21. NMR data are consistent with the reported literature.⁶²

2-(tert-Butylthio)thiazole (CD32). Silica gel column chromatography having eluent as *n*-hexane and ethyl acetate of 10:1 (v/v). Colorless oil. Yield: 162.8 mg, 94% (**Ni B-1**); 152.4 mg, 88% (**Pd B-1**). ESI-MS m/z $[\text{M} + \text{H}]^+ = 174.0193$ (calculated for $\text{C}_7\text{H}_{11}\text{NS}_2$, 174.0094). ^1H NMR (500 MHz, CDCl_3 , 300 K): δ (ppm): 7.78 (d, J = 3.40 Hz, 1H), 7.31 (d, J = 3.43 Hz, 1H), 1.38 (s, 9H). ^{13}C NMR (500 MHz, CDCl_3 , 300 K), δ (ppm): 160.39, 143.99, 122.72, 49.42, 30.94.

2-(Hexylthio)thiazole (CD33). Silica gel column chromatography having eluent as *n*-hexane and ethyl acetate of 10:1 (v/v). Colorless oil. Yield: 195.3 mg, 97% (**Ni B-1**); 189.2 mg, 94% (**Pd B-1**). ESI-MS m/z $[\text{M} + \text{H}]^+ = 202.0241$ (calculated for $\text{C}_9\text{H}_{15}\text{NS}_2$, 202.0176). ^1H NMR (500 MHz, CDCl_3 , 300 K): δ (ppm): 7.63 (d, J = 3.36 Hz, 1H), 7.18 (d, J = 3.38 Hz, 1H), 3.19 (t, J = 7.30 Hz, 2H), 1.72–1.75 (m, 2H), 1.41–1.44 (m, 2H), 1.29 (b, 4H), 0.87 (t, J = 6.84 Hz, 3H). ^{13}C NMR (500 MHz, CDCl_3 , 300 K), δ (ppm): 165.51, 142.79, 118.65, 34.72, 31.36, 29.29, 28.51, 22.59, 14.07.

2-(Decylthio)thiazole (CD34). Silica gel column chromatography having eluent as *n*-hexane and ethyl acetate of 10:1 (v/v). Colorless oil. Yield: 242.0 mg, 94% (**Ni B-1**); 234.2 mg, 91% (**Pd B-1**). ESI-MS m/z $[\text{M} + \text{H}]^+ = 258.0075$ (calculated for $\text{C}_{13}\text{H}_{23}\text{NS}_2$, 258.0034). ^1H NMR (500 MHz, CDCl_3 , 300 K): δ (ppm): 7.63 (d, J = 3.35 Hz, 1H), 7.17 (d, J = 3.37 Hz, 1H), 3.18 (t, J = 7.37 Hz, 2H), 1.76–1.70 (m, 2H), 1.43–1.39 (m, 2H), 1.24 (s, 12H), 0.86 (t, J = 6.87 Hz, 3H). ^{13}C NMR (500 MHz, CDCl_3 , 300 K), δ (ppm): 165.49, 142.77, 118.61, 34.69, 31.96, 29.59, 29.54, 29.37, 29.31, 29.17, 28.82, 22.75, 14.17.

1-(5-(tert-Butylthio)thiophen-2-yl)ethan-1-one (CD35). Silica gel column chromatography having eluent as *n*-hexane and ethyl acetate of 10:1 (v/v). Light brown solid. Yield: 207.9 mg, 97% (**Ni B-1**); 199.3 mg, 93% (**Pd B-1**). ESI-MS m/z $[\text{M} + \text{H}]^+ = 215.0066$ (calculated for $\text{C}_{10}\text{H}_{14}\text{OS}_2$, 215.0079). ^1H NMR (500 MHz, CDCl_3 , 300 K): δ (ppm): 7.59 (d, J = 3.77 Hz, 1H), 7.13 (d, J = 3.78 Hz, 1H), 2.52 (s, 3H), 1.34 (s, 9H). ^{13}C NMR (500 MHz, CDCl_3 , 300 K), δ (ppm): 190.18, 147.96, 142.41, 137.25, 132.30, 48.22, 30.85, 26.79.

1-(5-(Decylthio)thiophen-2-yl)ethan-1-one (CD36). Silica gel column chromatography having eluent as *n*-hexane and ethyl acetate of 10:1 (v/v). Light brown solid. Yield: 280.5 mg, 94% (**Ni B-1**); 271.6 mg, 91% (**Pd B-1**). ESI-MS m/z $[\text{M} + \text{H}]^+ = 299.0127$ (calculated for $\text{C}_{16}\text{H}_{26}\text{OS}_2$, 299.0093). ^1H NMR (500 MHz, CDCl_3 , 300 K): δ (ppm): 7.52 (d, 1H, J = 3.90 Hz), 6.96 (d, 1H, J = 3.91 Hz), 2.95 (t, 2H, J = 7.38 Hz), 2.50 (s, 3H), 1.64–1.71 (m, 2H), 1.37–1.41 (m, 2H), 1.25 (s, 12H), 0.87 (t, 3H, J = 6.90 Hz). ^{13}C NMR (500 MHz, CDCl_3 , 300 K), δ (ppm): 189.73, 148.42, 144.38, 132.97, 129.42, 37.49, 32.00, 29.63, 29.58, 29.40, 29.34, 29.20, 28.71, 26.44, 22.79, 14.22.

5-(Decylthio)-2-methylpyrimidin-4-ol (CD37). Silica gel column chromatography having eluent as *n*-hexane and ethyl acetate of 10:1 (v/v). White solid. Yield: 259.8 mg, 92% (**Ni B-1**); 240.0 mg, 85% (**Pd B-1**). ESI-MS m/z $[\text{M} + \text{H}]^+ = 283.0015$ (calculated for $\text{C}_{15}\text{H}_{26}\text{N}_2\text{OS}$, 283.0078). ^1H NMR (500 MHz, CDCl_3 , 300 K): δ (ppm): 13.31 (br, 1H), 6.10 (s, 1H), 2.94 (t, J = 7.37 Hz, 2H), 2.43 (s, 3H), 1.68–1.71 (m, 2H), 1.41–1.43 (m, 2H), 1.25 (b, 12H), 0.87 (t, J = 6.85 Hz, 3H). ^{13}C NMR (500 MHz, CDCl_3 , 300 K), δ (ppm): 171.38, 164.24, 158.11, 104.58, 32.01, 30.66, 29.65, 29.59, 29.41, 29.23, 29.00, 28.77, 22.79, 21.62, 14.22.

4-(Pyridin-4-ylthio)phenol (CD38). Silica gel column chromatography having eluent as *n*-hexane and ethyl acetate of 5:1 (v/v). Light brown solid. Yield: 203.1 mg, 92% (**Ni B-1**); 174.8 mg, 86% (**Pd B-1**). ESI-MS m/z $[\text{M} + \text{H}]^+ = 204.0067$ (calculated for $\text{C}_{11}\text{H}_9\text{NOS}$, 204.0024). ^1H NMR (500 MHz, CDCl_3 , 300 K): δ (ppm): 8.38 (br, 2H), 7.35 (t, J = 8.03 Hz, 2H), 7.17 (d, J = 7.43 Hz, 1H), 7.02 (d, J = 7.63 Hz, 2H), 6.76 (d, J = 6.11 Hz, 2H). ^{13}C NMR (500 MHz, CDCl_3 , 300 K), δ (ppm): 165.00, 154.14, 151.40, 130.34, 125.59, 120.95, 112.34.

1-(4-(Pyridin-4-ylthio)phenyl)ethan-1-one (**CD39**). Silica gel column chromatography having eluent as *n*-hexane and ethyl acetate of 5:1 (v/v). Light gray solid. Yield: 217.8 mg, 95% (**Ni B-1**); 204.0 mg, 89% (**Pd B-1**). ESI-MS m/z $[M + H]^+$ = 230.0157 (calculated for $C_{13}H_{11}NOS$, 230.0086). 1H NMR (500 MHz, $CDCl_3$, 300 K): δ (ppm): 8.42 (s, 2H), 7.97 (d, 2H, J = 8.31 Hz), 7.56 (d, 2H, J = 8.31 Hz), 7.06 (s, 2H), 2.62 (s, 3H). ^{13}C NMR (500 MHz, $CDCl_3$, 300 K), δ (ppm): 197.15, 149.96, 147.92, 137.28, 137.11, 133.50, 129.57, 122.51, 26.75. NMR data are consistent with the reported literature.⁶³

4-((4-Nitrophenyl)thio)pyridine (**CD40**). Silica gel column chromatography having eluent as *n*-hexane and ethyl acetate of 5:1 (v/v). Light brown solid. Yield: 216.0 mg, 93% (**Ni B-1**); 209.0 mg, 90% (**Pd B-1**). ESI-MS m/z $[M + H]^+$ = 233.059 (calculated for $C_{11}H_8N_2O_2S$, 233.0042). 1H NMR (500 MHz, $CDCl_3$, 300 K): δ (ppm): 8.11 (d, J = 9.43 Hz, 2H), 7.40 (d, J = 8.70 Hz, 2H), 6.60 (d, J = 9.44 Hz, 2H), 6.46 (d, J = 8.69 Hz, 2H). ^{13}C NMR (500 MHz, $CDCl_3$, 300 K), δ (ppm): 154.36, 146.22, 138.04, 126.24, 117.42, 110.37. NMR data are consistent with the reported literature.⁶⁴

4-(Pyridin-4-ylthio)benzonitrile (**CD41**). Silica gel column chromatography having eluent as *n*-hexane and ethyl acetate of 5:1 (v/v). White solid. Yield: 203.7 mg, 96% (**Ni B-1**); 191.0 mg, 90% (**Pd B-1**). ESI-MS m/z $[M + H]^+$ = 213.0107 (calculated for $C_{12}H_8N_2S$, 213.0043). 1H NMR (500 MHz, $CDCl_3$, 300 K): δ (ppm): 8.47 (d, J = 5.47 Hz, 1H), 7.66 (d, J = 8.39 Hz, 1H), 7.53 (d, J = 8.36 Hz, 1H), 7.10 (d, J = 6.09 Hz, 1H). ^{13}C NMR (500 MHz, $CDCl_3$, 300 K), δ (ppm): 150.20, 146.49, 138.40, 133.21, 133.07, 123.30, 118.14, 112.42. NMR data are consistent with the reported literature.¹⁸

■ ASSOCIATED CONTENT

Supporting Information

The Supporting Information is available free of charge at <https://pubs.acs.org/doi/10.1021/acs.organomet.0c00732>.

Unit cell representation, crystal data, 1H NMR and ^{13}C NMR spectra of ligands, 1H NMR and ^{13}C NMR spectra of C–S cross-coupled compounds (PDF)

Accession Codes

CCDC 2038719–2038722 contain the supplementary crystallographic data for this paper. These data can be obtained free of charge via www.ccdc.cam.ac.uk/data_request/cif, or by emailing data_request@ccdc.cam.ac.uk, or by contacting The Cambridge Crystallographic Data Centre, 12 Union Road, Cambridge CB2 1EZ, UK; fax: +44 1223 336033.

■ AUTHOR INFORMATION

Corresponding Author

Mihaela C. Stefan – Department of Chemistry and Biochemistry, University of Texas at Dallas, Richardson, Texas 75080, United States; orcid.org/0000-0003-2475-4635; Phone: 972-883-6581; Email: mihaela@utdallas.edu

Authors

Md Muktadir Talukder – Department of Chemistry and Biochemistry, University of Texas at Dallas, Richardson, Texas 75080, United States

Justin T. Miller – Department of Chemistry and Biochemistry, University of Texas at Dallas, Richardson, Texas 75080, United States

John Michael O. Cue – Department of Chemistry and Biochemistry, University of Texas at Dallas, Richardson, Texas 75080, United States

Chinthaka M. Udamulle – Department of Chemistry and Biochemistry, University of Texas at Dallas, Richardson, Texas 75080, United States

Abhi Bhadran – Department of Chemistry and Biochemistry, University of Texas at Dallas, Richardson, Texas 75080, United States

Michael C. Biewer – Department of Chemistry and Biochemistry, University of Texas at Dallas, Richardson, Texas 75080, United States

Complete contact information is available at:

<https://pubs.acs.org/doi/10.1021/acs.organomet.0c00732>

Notes

The authors declare no competing financial interest.

■ ACKNOWLEDGMENTS

Financial support provided by the National Science Foundation (CHE-1609880 and CHE-1566059) and Welch Foundation (AT1740) is gratefully acknowledged. M.C.S. is thankful for the generous endowed chair support from the Eugene McDermott Foundation. We thank Dr. Gregory T. McCandless for collecting the crystal structure data.

■ REFERENCES

- (1) Hartwig, J. F. Carbon-Heteroatom Bond-Forming Reductive Eliminations of Amines, Ethers, and Sulfides. *Acc. Chem. Res.* **1998**, *31*, 852–860.
- (2) Hartwig, J. F. Carbon-heteroatom bond formation catalysed by organometallic complexes. *Nature* **2008**, *455*, 314–322.
- (3) Jiang, M.; Li, H.; Yang, H.; Fu, H. Room-Temperature Arylation of Thiols: Breakthrough with Aryl Chlorides. *Angew. Chem., Int. Ed.* **2017**, *56*, 874–879.
- (4) Lee, C.-F.; Liu, Y.-C.; Badsara, S. S. Transition-Metal-Catalyzed C–S Bond Coupling Reaction. *Chem. - Asian J.* **2014**, *9*, 706–722.
- (5) Migita, T.; Shimizu, T.; Asami, Y.; Shiobara, J.-i.; Kato, Y.; Kosugi, M. The Palladium Catalyzed Nucleophilic Substitution of Aryl Halides by Thiolate Anions. *Bull. Chem. Soc. Jpn.* **1980**, *53*, 1385–1389.
- (6) Kosugi, M.; Ogata, T.; Terada, M.; Sano, H.; Migita, T. Palladium-catalyzed Reaction of Stannyl Sulfide with Aryl Bromide. Preparation of Aryl Sulfide. *Bull. Chem. Soc. Jpn.* **1985**, *58*, 3657–3658.
- (7) Alvaro, E.; Hartwig, J. F. Resting State and Elementary Steps of the Coupling of Aryl Halides with Thiols Catalyzed by Alkylbisphosphine Complexes of Palladium. *J. Am. Chem. Soc.* **2009**, *131*, 7858–7868.
- (8) Scatollin, T.; Senol, E.; Yin, G.; Guo, Q.; Schoenebeck, F. Site-Selective C–S Bond Formation at C–Br over C–OTf and C–Cl Enabled by an Air-Stable, Easily Recoverable, and Recyclable Palladium(I) Catalyst. *Angew. Chem., Int. Ed.* **2018**, *57*, 12425–12429.
- (9) Hartwig, J. F. Evolution of a Fourth Generation Catalyst for the Amination and Thioetherification of Aryl Halides. *Acc. Chem. Res.* **2008**, *41*, 1534–1544.
- (10) Mann, G.; Baranano, D.; Hartwig, J. F.; Rheingold, A. L.; Guzei, I. A. Carbon-Sulfur Bond-Forming Reductive Elimination Involving sp^2 , sp^2 , and sp^3 -Hybridized Carbon. Mechanism, Steric Effects, and Electronic Effects on Sulfide Formation. *J. Am. Chem. Soc.* **1998**, *120*, 9205–9219.
- (11) Fernández-Rodríguez, M. A.; Shen, Q.; Hartwig, J. F. A General and Long-Lived Catalyst for the Palladium-Catalyzed Coupling of Aryl Halides with Thiols. *J. Am. Chem. Soc.* **2006**, *128*, 2180–2181.
- (12) Fernández-Rodríguez, M. A.; Shen, Q.; Hartwig, J. F. Highly Efficient and Functional-Group-Tolerant Catalysts for the Palladium-Catalyzed Coupling of Aryl Chlorides with Thiols. *Chem. - Eur. J.* **2006**, *12*, 7782–7796.
- (13) Valente, C.; Pompeo, M.; Sayah, M.; Organ, M. G. Carbon-Heteroatom Coupling Using Pd-PEPPSI Complexes. *Org. Process Res. Dev.* **2014**, *18*, 180–190.

- (14) Xu, J.; Liu, R. Y.; Yeung, C. S.; Buchwald, S. L. Monophosphine Ligands Promote Pd-Catalyzed C-S Cross-Coupling Reactions at Room Temperature with Soluble Bases. *ACS Catal.* **2019**, *9*, 6461–6466.
- (15) Bastug, G.; Nolan, S. P. Carbon-Sulfur Bond Formation Catalyzed by [Pd(IPr*OMe)(cin)Cl] (cin = cinnamyl). *J. Org. Chem.* **2013**, *78*, 9303–9308.
- (16) Fernández-Rodríguez, M. A.; Hartwig, J. F. A General, Efficient, and Functional-Group-Tolerant Catalyst System for the Palladium-Catalyzed Thioetherification of Aryl Bromides and Iodides. *J. Org. Chem.* **2009**, *74*, 1663–1672.
- (17) Mohammadinezhad, A.; Akhlaghinia, B. CoII immobilized on an aminated magnetic metal-organic framework catalyzed C-N and C-S bond forming reactions: a journey for the mild and efficient synthesis of arylamines and arylsulfides. *New J. Chem.* **2019**, *43*, 15525–15538.
- (18) Wang, Y.; Deng, L.; Wang, X.; Wu, Z.; Wang, Y.; Pan, Y. Electrochemically Promoted Nickel-Catalyzed Carbon-Sulfur Bond Formation. *ACS Catal.* **2019**, *9*, 1630–1634.
- (19) Venkanna, G. T.; Arman, H. D.; Tonzetich, Z. J. Catalytic C-S Cross-Coupling Reactions Employing Ni Complexes of Pyrrole-Based Pincer Ligands. *ACS Catal.* **2014**, *4*, 2941–2950.
- (20) Gehrtz, P. H.; Geiger, V.; Schmidt, T.; Sršan, L.; Fleischer, I. Cross-Coupling of Chloro(hetero)arenes with Thiolates Employing a Ni(0)-Precatalyst. *Org. Lett.* **2019**, *21*, 50–55.
- (21) Zhang, J.; Medley, C. M.; Krause, J. A.; Guan, H. Mechanistic Insights into C-S Cross-Coupling Reactions Catalyzed by Nickel Bis(phosphinite) Pincer Complexes. *Organometallics* **2010**, *29*, 6393–6401.
- (22) Sikari, R.; Sinha, S.; Das, S.; Saha, A.; Chakraborty, G.; Mondal, R.; Paul, N. D. Achieving Nickel Catalyzed C-S Cross-Coupling under Mild Conditions Using Metal-Ligand Cooperativity. *J. Org. Chem.* **2019**, *84*, 4072–4085.
- (23) Jones, K. D.; Power, D. J.; Bierer, D.; Gericke, K. M.; Stewart, S. G. Nickel Phosphite/Phosphine-Catalyzed C-S Cross-Coupling of Aryl Chlorides and Thiols. *Org. Lett.* **2018**, *20*, 208–211.
- (24) Xu, X.-B.; Liu, J.; Zhang, J.-J.; Wang, Y.-W.; Peng, Y. Nickel-Mediated Inter- and Intramolecular C-S Coupling of Thiols and Thioacetates with Aryl Iodides at Room Temperature. *Org. Lett.* **2013**, *15*, 550–553.
- (25) Oderinde, M. S.; Frenette, M.; Robbins, D. W.; Aquila, B.; Johannes, J. W. Photoredox Mediated Nickel Catalyzed Cross-Coupling of Thiols With Aryl and Heteroaryl Iodides via Thiyl Radicals. *J. Am. Chem. Soc.* **2016**, *138*, 1760–1763.
- (26) Kabir, M. S.; Lorenz, M.; Van Linn, M. L.; Namjoshi, O. A.; Ara, S.; Cook, J. M. A Very Active Cu-Catalytic System for the Synthesis of Aryl, Heteroaryl, and Vinyl Sulfides. *J. Org. Chem.* **2010**, *75*, 3626–3643.
- (27) Panova, Y. S.; Kashin, A. S.; Vorobev, M. G.; Degtyareva, E. S.; Ananikov, V. P. Nature of the Copper-Oxide-Mediated C-S Cross-Coupling Reaction: Leaching of Catalytically Active Species from the Metal Oxide Surface. *ACS Catal.* **2016**, *6*, 3637–3643.
- (28) Uyeda, C.; Tan, Y.; Fu, G. C.; Peters, J. C. A New Family of Nucleophiles for Photoinduced, Copper-Catalyzed Cross-Couplings via Single-Electron Transfer: Reactions of Thiols with Aryl Halides Under Mild Conditions (0 °C). *J. Am. Chem. Soc.* **2013**, *135*, 9548–9552.
- (29) Timpa, S. D.; Pell, C. J.; Ozerov, O. V. A Well-Defined (POCOP)Rh Catalyst for the Coupling of Aryl Halides with Thiols. *J. Am. Chem. Soc.* **2014**, *136*, 14772–14779.
- (30) Reddy, V. P.; Swapna, K.; Kumar, A. V.; Rao, K. R. Indium-Catalyzed C-S Cross-Coupling of Aryl Halides with Thiols. *J. Org. Chem.* **2009**, *74*, 3189–3191.
- (31) Guo, F.-J.; Sun, J.; Xu, Z.-Q.; Kühn, F. E.; Zang, S.-L.; Zhou, M.-D. C-S cross-coupling of aryl halides with alkyl thiols catalyzed by in-situ generated nickel(II) N-heterocyclic carbene complexes. *Catal. Commun.* **2017**, *96*, 11–14.
- (32) Lan, M.-T.; Wu, W.-Y.; Huang, S.-H.; Luo, K.-L.; Tsai, F.-Y. Reusable and efficient CoCl₂·6H₂O/cationic 2,2'-bipyridyl system-catalyzed S-arylation of aryl halides with thiols in water under air. *RSC Adv.* **2011**, *1*, 1751–1755.
- (33) Liu, Y.; Huang, B.; Cao, X.; Wu, D.; Wan, J.-P. Synthesis of heteroaryl containing sulfides via enaminone ligand assisted, copper-catalyzed C-S coupling reactions of heteroaryl thiols and aryl halides. *RSC Adv.* **2014**, *4*, 37733–37737.
- (34) Talukder, M. M.; Cue, J. M. O.; Miller, J. T.; Gamage, P. L.; Aslam, A.; McCandless, G. T.; Biewer, M. C.; Stefan, M. C. Ligand Steric Effects of α -Diimine Nickel(II) and Palladium(II) Complexes in the Suzuki-Miyaura Cross-Coupling Reaction. *ACS Omega* **2020**, *5*, 24018–24032.
- (35) Gates, D. P.; Svejda, S. A.; Oñate, E.; Killian, C. M.; Johnson, L. K.; White, P. S.; Brookhart, M. Synthesis of Branched Polyethylene Using (α -Diimine)nickel(II) Catalysts: Influence of Temperature, Ethylene Pressure, and Ligand Structure on Polymer Properties. *Macromolecules* **2000**, *33*, 2320–2334.
- (36) Rhinehart, J. L.; Brown, L. A.; Long, B. K. A Robust Ni(II) α -Diimine Catalyst for High Temperature Ethylene Polymerization. *J. Am. Chem. Soc.* **2013**, *135*, 16316–16319.
- (37) Zhong, L.; Li, G.; Liang, G.; Gao, H.; Wu, Q. Enhancing Thermal Stability and Living Fashion in α -Diimine-Nickel-Catalyzed (Co)polymerization of Ethylene and Polar Monomer by Increasing the Steric Bulk of Ligand Backbone. *Macromolecules* **2017**, *50*, 2675–2682.
- (38) Popeney, C.; Guan, Z. Ligand Electronic Effects on Late Transition Metal Polymerization Catalysts. *Organometallics* **2005**, *24*, 1145–1155.
- (39) Falivene, L.; Credendino, R.; Poater, A.; Petta, A.; Serra, L.; Oliva, R.; Scarano, V.; Cavallo, L. SambVca 2. A Web Tool for Analyzing Catalytic Pockets with Topographic Steric Maps. *Organometallics* **2016**, *35*, 2286–2293.
- (40) Falivene, L.; Cao, Z.; Petta, A.; Serra, L.; Poater, A.; Oliva, R.; Scarano, V.; Cavallo, L. Towards the online computer-aided design of catalytic pockets. *Nat. Chem.* **2019**, *11*, 872–879.
- (41) Marcone, J. E.; Moloy, K. G. Kinetic Study of Reductive Elimination from the Complexes (Diphosphine)Pd(R)(CN). *J. Am. Chem. Soc.* **1998**, *120*, 8527–8528.
- (42) Crumpton-Bregel, D. M.; Goldberg, K. I. Mechanisms of C-C and C-H Alkane Reductive Eliminations from Octahedral Pt(IV): Reaction via Five-Coordinate Intermediates or Direct Elimination? *J. Am. Chem. Soc.* **2003**, *125*, 9442–9456.
- (43) Gallardo, I.; Guirado, G.; Marquet, J. Electrochemical Synthesis of Alkyl Nitroaromatic Compounds. *J. Org. Chem.* **2003**, *68*, 631–633.
- (44) Yang, C.; Williams, J. M. Palladium-Catalyzed Cyanation of Aryl Bromides Promoted by Low-Level Organotin Compounds. *Org. Lett.* **2004**, *6*, 2837–2840.
- (45) Shi, Y.; Guo, H.; Qin, M.; Wang, Y.; Zhao, J.; Sun, H.; Wang, H.; Wang, Y.; Zhou, X.; Facchetti, A.; Lu, X.; Zhou, M.; Guo, X. Imide-Functionalized Thiazole-Based Polymer Semiconductors: Synthesis, Structure-Property Correlations, Charge Carrier Polarity, and Thin-Film Transistor Performance. *Chem. Mater.* **2018**, *30*, 7988–8001.
- (46) McCulloch, B.; Ho, V.; Hoarfrost, M.; Stanley, C.; Do, C.; Heller, W. T.; Segalman, R. A. Polymer Chain Shape of Poly(3-alkylthiophenes) in Solution Using Small-Angle Neutron Scattering. *Macromolecules* **2013**, *46*, 1899–1907.
- (47) Cui, C.; Wong, W.-Y.; Li, Y. Improvement of open-circuit voltage and photovoltaic properties of 2D-conjugated polymers by alkylthio substitution. *Energy Environ. Sci.* **2014**, *7*, 2276–2284.
- (48) Sheldrick, G. M. SHELXT-Integrated Space-Group and Crystalstructure Determination. *Acta Crystallogr., Sect. A: Found. Adv.* **2015**, *71*, 3–8.
- (49) Sheldrick, G. M. Crystal Structure Refinement with SHELXL. *Acta Crystallogr., Sect. C: Struct. Chem.* **2015**, *71*, 3–8.
- (50) Sreenath, K.; Yuan, Z.; Macias-Contreras, M.; Ramachandran, V.; Clark, R. J.; Zhu, L. Dual Role of Acetate in Copper(II) Acetate Catalyzed Dehydrogenation of Chelating Aromatic Secondary Amines: A Kinetic Case Study of Copper-Catalyzed Oxidation Reactions. *Eur. J. Inorg. Chem.* **2016**, *2016*, 3728–3743.

- (51) Song, G.; Guo, L.; Du, Q.; Kong, W.; Li, W.; Liu, Z. Highly active mono and bis-ligated iminopyridyl nickel catalysts for 1-hexene reactions. *J. Organomet. Chem.* **2018**, 858, 1–7.
- (52) Sorribes, I.; Corma, A. Nanolayered cobalt-molybdenum sulphides (Co-Mo-S) catalyse borrowing hydrogen C-S bond formation reactions of thiols or H₂S with alcohols. *Chem. Sci.* **2019**, 10, 3130–3142.
- (53) Ren, X.; Tang, S.; Li, L.; Li, J.; Liang, H.; Li, G.; Yang, G.; Li, H.; Yuan, B. Surfactant-Type Catalyst for Aerobic Oxidative Coupling of Hydrazine with Thiol in Water. *J. Org. Chem.* **2019**, 84, 8683–8690.
- (54) Vantourout, J. C.; Miras, H. N.; Isidro-Llobet, A.; Sproules, S.; Watson, A. J. B. Spectroscopic Studies of the Chan-Lam Amination: A Mechanism-Inspired Solution to Boronic Ester Reactivity. *J. Am. Chem. Soc.* **2017**, 139, 4769–4779.
- (55) Ko, J.; Ham, J.; Yang, I.; Chin, J.; Nam, S.-J.; Kang, H. A simple one-pot synthesis of hydroxylated and carboxylated aryl alkyl sulfides from various bromobenzenes. *Tetrahedron Lett.* **2006**, 47, 7101–7106.
- (56) Wang, L.; Zhou, W.-Y.; Chen, S.-C.; He, M.-Y.; Chen, Q. A Highly Efficient Palladium-Catalyzed One-Pot Synthesis of Unsymmetrical Aryl Alkyl Thioethers under Mild Conditions in Water. *Adv. Synth. Catal.* **2012**, 354, 839–845.
- (57) Gholinejad, M. One-Pot Copper-Catalysed Thioetherification of Aryl Halides Using Alcohols and Lawesson's Reagent in Diglyme. *Eur. J. Org. Chem.* **2015**, 2015, 4162–4167.
- (58) Zhao, J.-N.; Kayumov, M.; Wang, D.-Y.; Zhang, A. Transition-Metal-Free Aryl-Heteroatom Bond Formation via C-S Bond Cleavage. *Org. Lett.* **2019**, 21, 7303–7306.
- (59) Jouffroy, M.; Kelly, C. B.; Molander, G. A. Thioetherification via Photoredox/Nickel Dual Catalysis. *Org. Lett.* **2016**, 18, 876–879.
- (60) Di Maria, F.; Olivelli, P.; Gazzano, M.; Zanelli, A.; Biasiucci, M.; Gigli, G.; Gentili, D.; D'Angelo, P.; Cavallini, M.; Barbarella, G. A Successful Chemical Strategy To Induce Oligothiophene Self-Assembly into Fibers with Tunable Shape and Function. *J. Am. Chem. Soc.* **2011**, 133, 8654–8661.
- (61) Oyaizu, K.; Iwasaki, T.; Tsukahara, Y.; Tsuchida, E. Linear Ladder-Type π -Conjugated Polymers Composed of Fused Thiophene Ring Systems. *Macromolecules* **2004**, 37, 1257–1270.
- (62) Yonekura, K.; Yoshimura, Y.; Akehi, M.; Tsuchimoto, T. A Heteroarylamine Library: Indium-Catalyzed Nucleophilic Aromatic Substitution of Alkoxyheteroarenes with Amines. *Adv. Synth. Catal.* **2018**, 360, 1159–1181.
- (63) Liu, B.; Lim, C.-H.; Miyake, G. M. Visible-Light-Promoted C-S Cross-Coupling via Intermolecular Charge Transfer. *J. Am. Chem. Soc.* **2017**, 139, 13616–13619.
- (64) Moser, D.; Duan, Y.; Wang, F.; Ma, Y.; O'Neill, M. J.; Cornella, J. Selective Functionalization of Aminoheterocycles by a Pyrylium Salt. *Angew. Chem., Int. Ed.* **2018**, 57, 11035–11039.